

APPENDIX A: IMAGES FROM KYEN KNIGHT'S THESIS

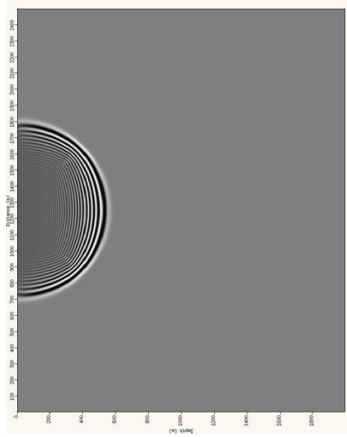


Figure 5.6.1a: Simulation of a seismic wave at 0.1 sec, emitted from source at 1250 m.

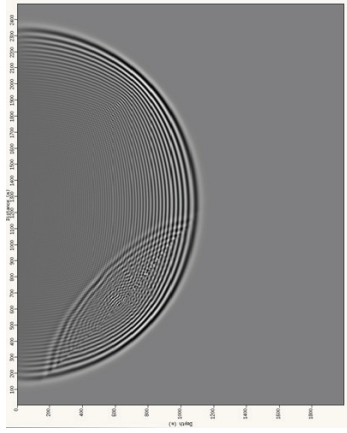


Figure 5.6.1b: Seismic wave at 0.2 sec, reflecting from the Mount Black Fault.

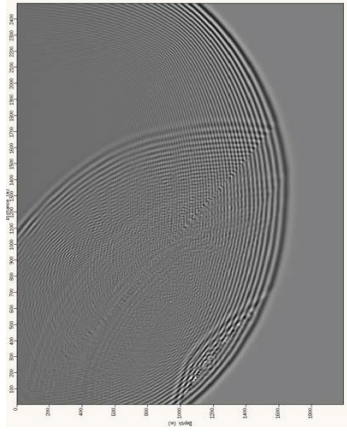


Figure 5.6.1c: Seismic wave at 0.3 sec, wave front reaches the Rosebery fault. Reflections from the Mt Black fault recorded at the surface.

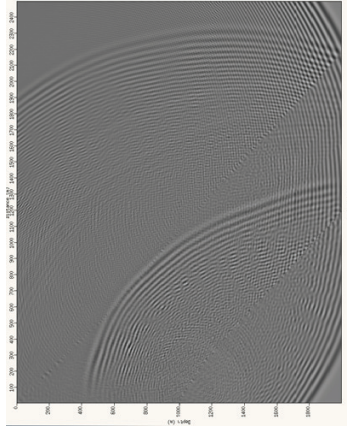


Figure 5.6.1d: Seismic wave at 0.4 sec, weak reflections from the mine sequence (Black Shale-Footwall) are recorded at the surface.

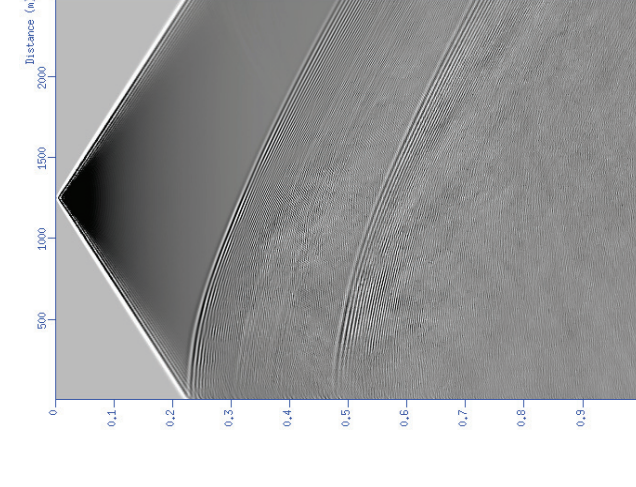


Figure 5.6.2: Synthetic seismogram derived from a seismic source at 1250m through a conceptual geologic model. Two strong reflections from fault rocks appear prominently, with weak reflections from mine sequence occurring between fault reflections

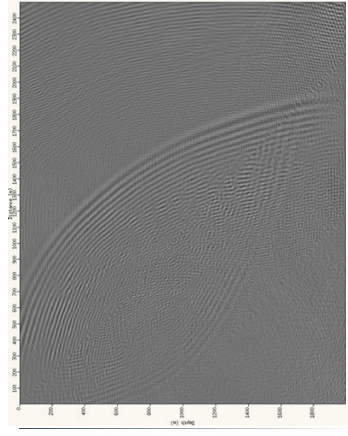


Figure 5.6.1e: Seismic wave at 0.5 sec, reflections from the Rosebery fault are recorded at surface

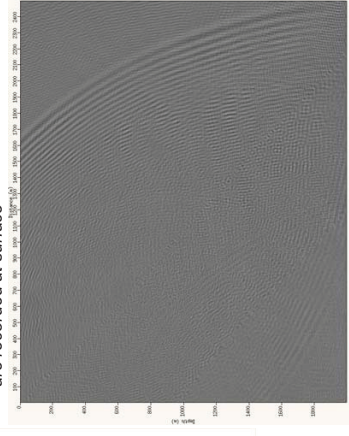


Figure 5.6.1f: Seismic wave at 0.6 sec, reflections from Rosebery fault continue to be recorded at the surface

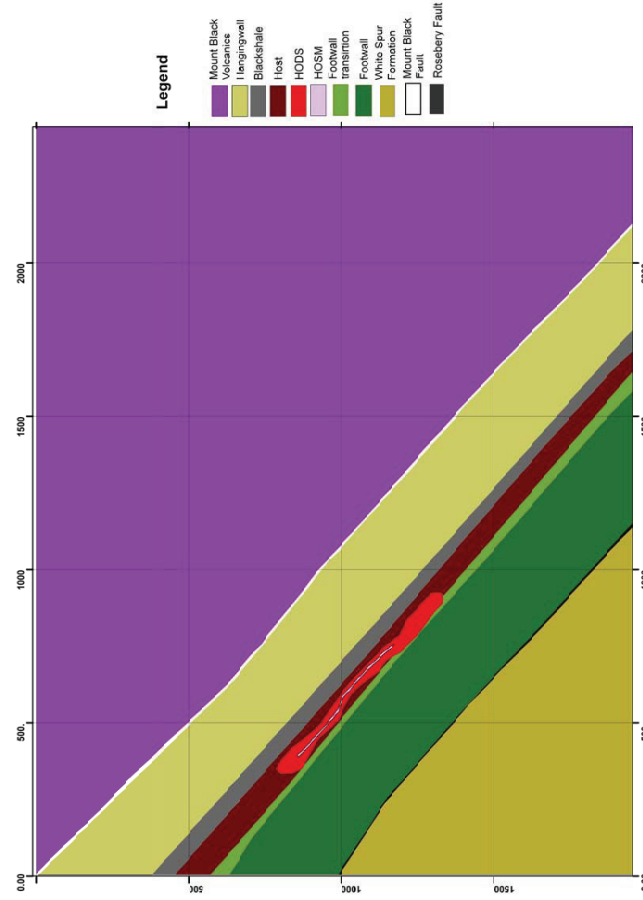


Figure 5.6.3: Cross-sectional view of conceptual geological model of the north Rosebery mine sequence.

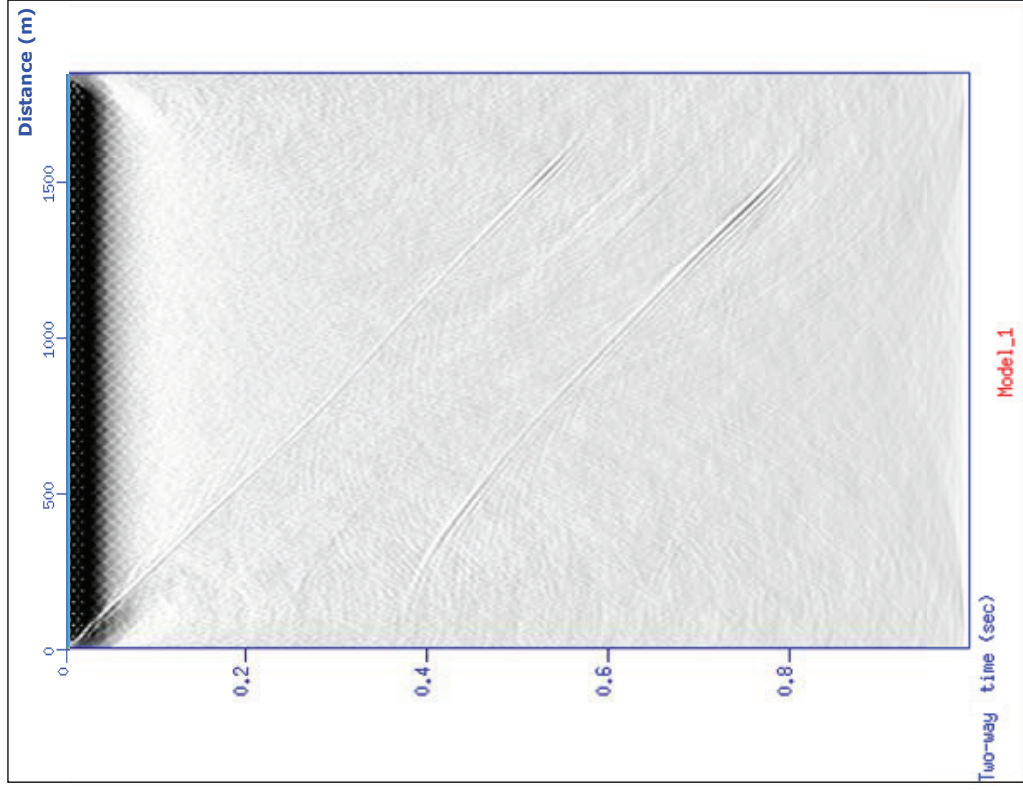


Figure 5.6.4a: A synthetic seismic section derived from a conceptual geological model of the Rosebery mine sequence, with axes showing distance and two way time. The seismic section has been processed using NMO, migration, amplitude gain and frequency filtering, and has been amplitude clipped to the top 1 percentile of amplitudes. Processing input parameters below.

NMO correction, v_{nmo}=5700
 Migration, v_{mig}=5700
 Gain, g_{pow}=0.5
 Filter, low pass 0, 100, 150, 500 (amps 1,1,0,0)

Figure 5.6.4b: Synthetic seismic section with background noise added prior to processing. A signal to noise ratio of 200 obscures reflections from the mine sequence

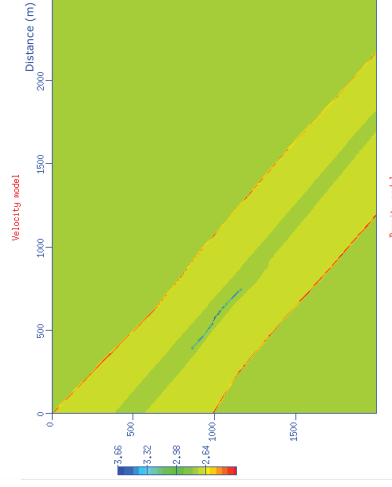
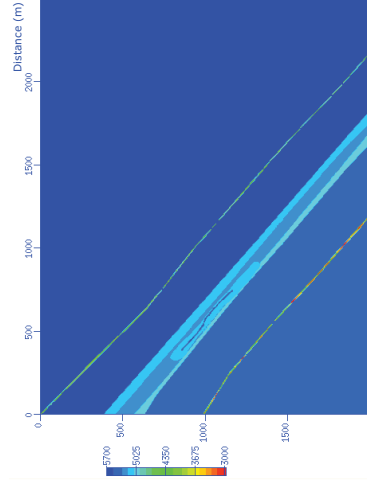


Figure 5.6.4c : Input velocity (top) and density models (above), developed for finite differencing modelling. Faults and mine sequence Black Shale and Host rock units show significant contrasts in both density and velocity

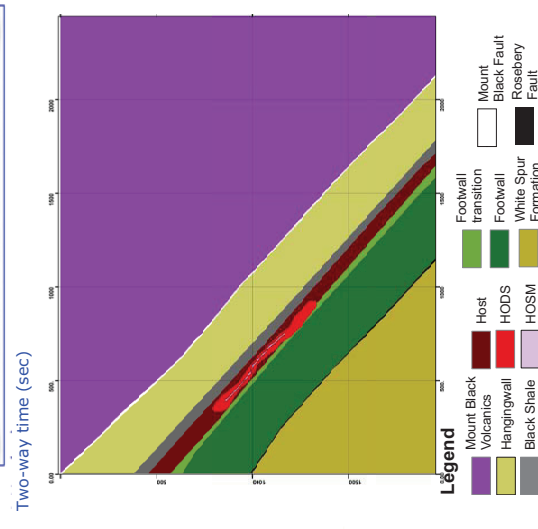
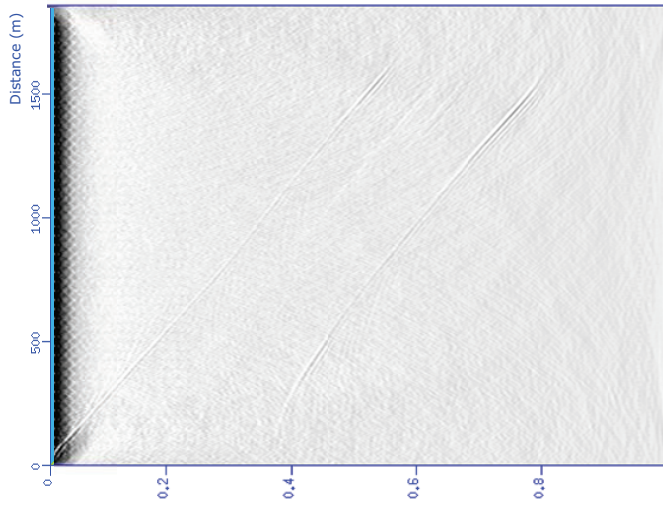


Figure 5.6.4d: A Conceptual geological model of the Rosebery mine sequence.

HODS = Host Rock disseminated mineralisation
 HOSM = Host Rock semi-massive mineralisation

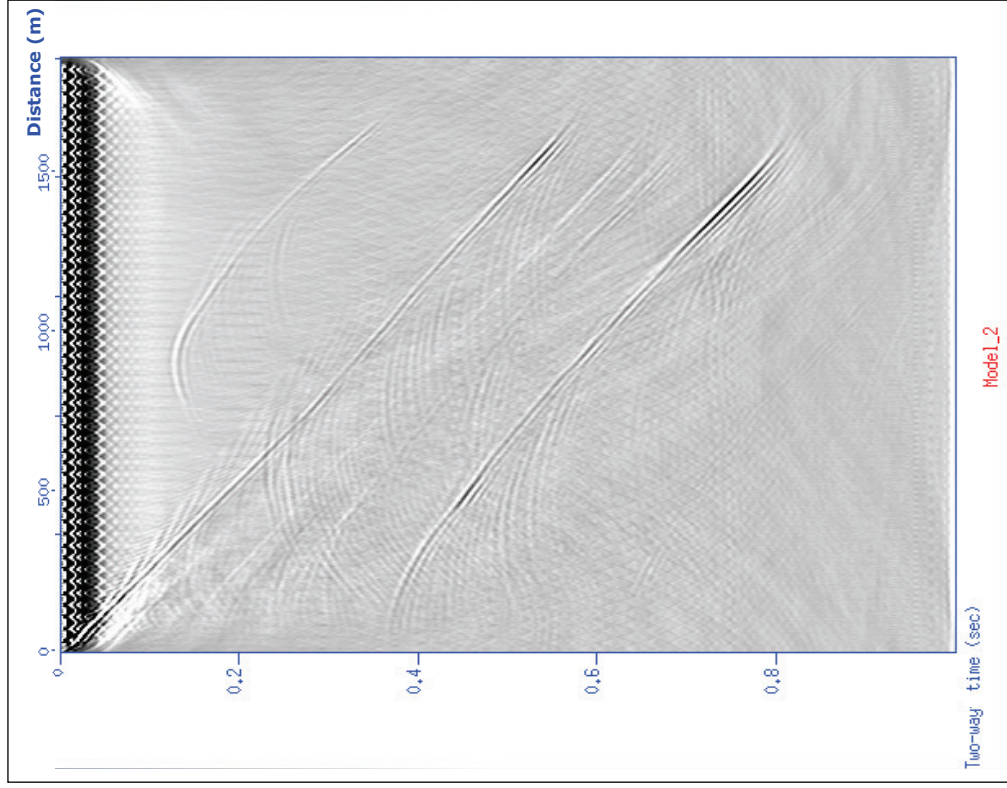


Figure 5.6.5a: A synthetic seismic section derived from a conceptual geological model of the Rosebery mine sequence, with axes showing distance and two way time. The section has been processed using NMO corrections, migration, amplitude gain, frequency filtering, and has been amplitude clipped to the top 1 percentile of amplitudes. Strong reflections from fault rocks and a carbonate rock unit are clearly visualised, with weak reflections from the mine sequence between faults. Processing input parameters below.

NMO correction, v_{nmo}=5700
 Migration, v_{mig}=5700
 Gain, g_{pow}=0.5
 Filter, low pass 0, 100, 150, 500 (amps 1, 1, 0, 0)

Figure 5.6.5b: Synthetic seismic section with background noise added prior to processing. A signal to noise ratio of 200 obscures the reflections from mine sequence

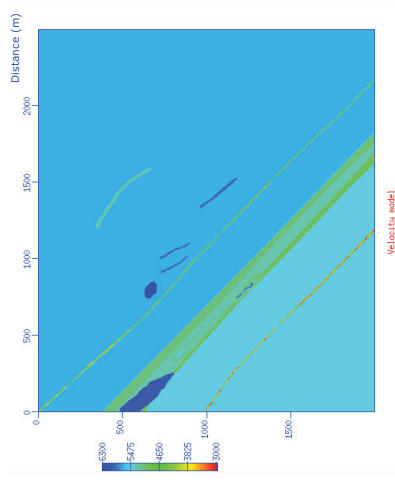


Figure 5.6.5c: Input velocity (top) and density models (above), developed for finite differencing modelling, showing velocity contrasts of intrusive units and massive banded ore rocks and density contrasts of fault rocks and banded ores

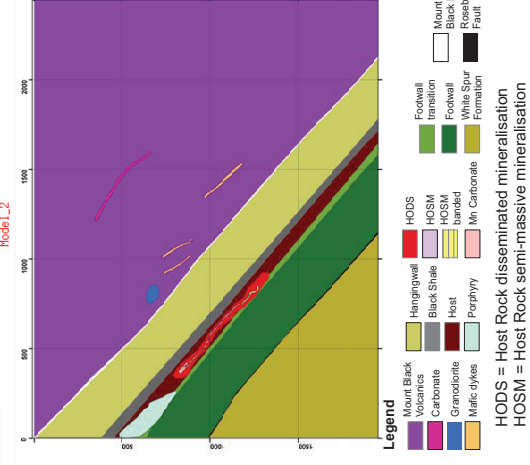
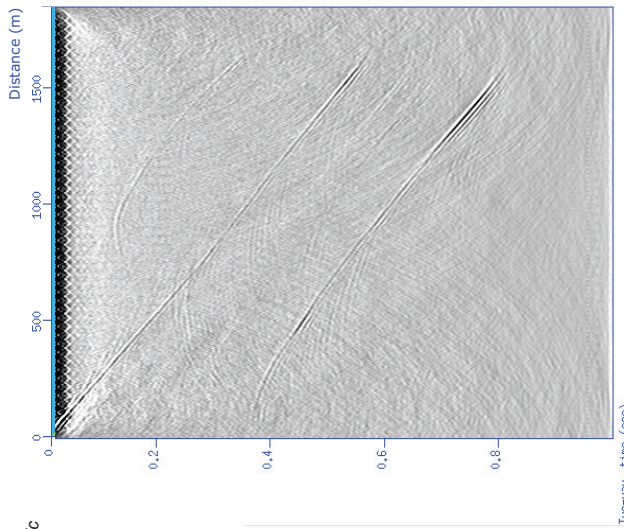
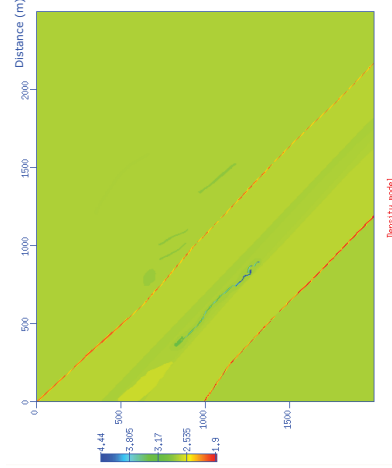


Figure 5.6.5d: Conceptual geological model of the Rosebery mine sequence with additional intrusive rock units, massive banded ores and Mn-carbonate

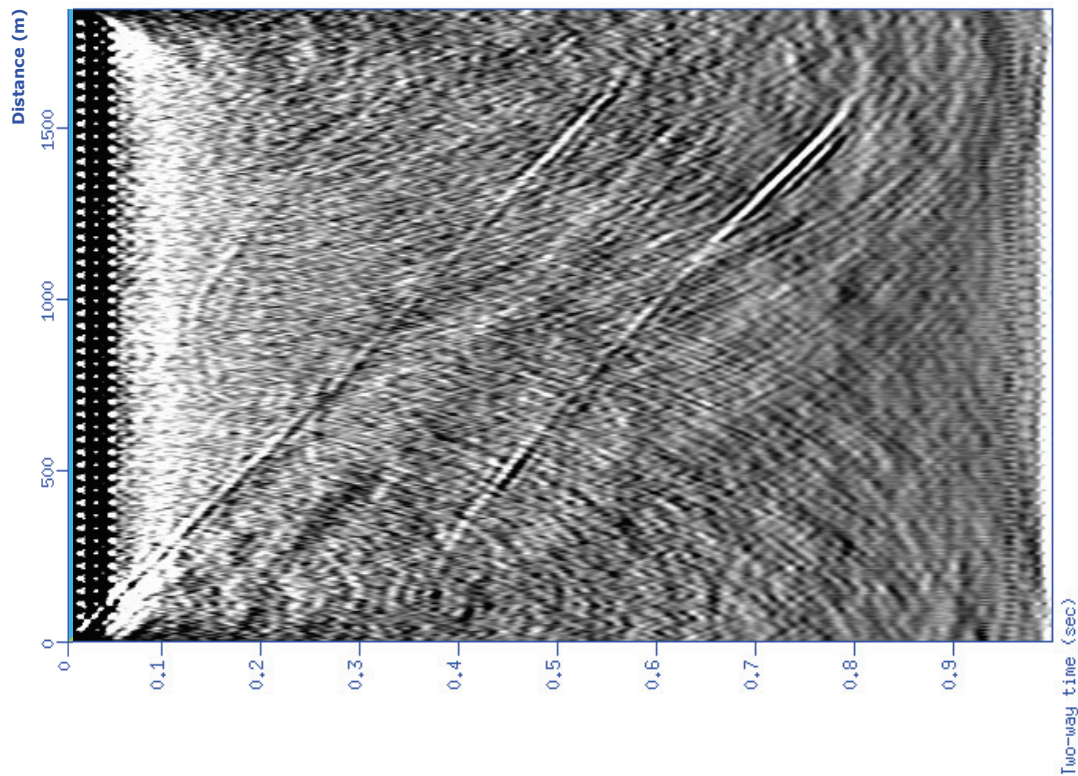
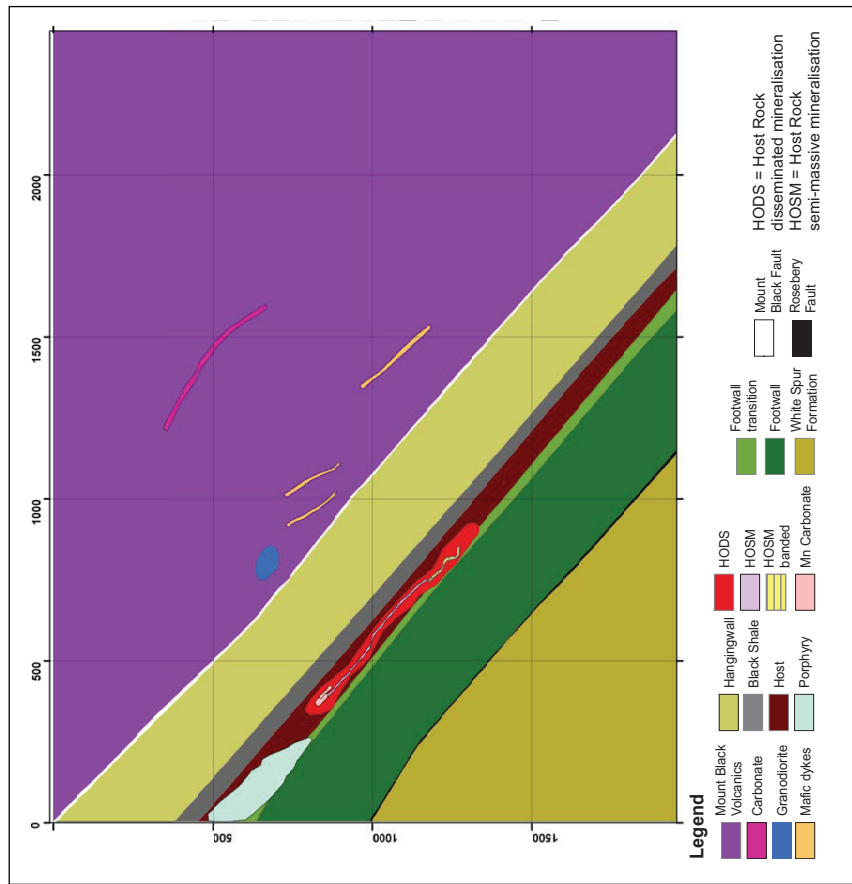
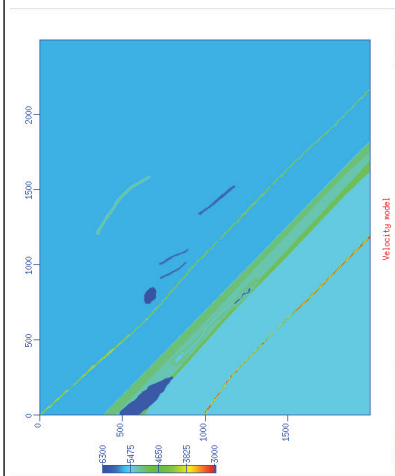


Figure 5.6.6a: A synthetic seismic section derived from a conceptual geological model the Rosebery mine sequence, with axes showing distance and two way time. The section has been low pass frequency filtered removing reflections with frequencies below 100 Hz, and has been amplitude clipped to the top 5th percentile of amplitudes. Processing input parameters below.

NMO, v_{nm0}=5700 Migration, v_{mig}=5700
 Gain, gpow=0.5 Filter, low pass 0.80, 100, 500 (amps 1, 1, 0, 0)



Figures 5.6.6b and c: Conceptual geological model (top) of the Rosebery mine sequence with additional intrusive rock units, massive banded ores and Mn-carbonate. An input velocity model (left), developed for finite differencing modelling, showing velocity contrasts of intrusive units and massive banded ore rocks.



APPENDIX B: HISEIS ACQUISITION REPORT

HiSeis Pty Ltd.
Suite 4, Enterprise Unit 3
9 De Laeter Way
Bentley WA 6102
Australia



Acquisition Report

*Rosebery, Tasmania
February – August 2012*

For

Minerals and Metals Group Ltd.

Report number:

MMG-3DROSEACQ12

Prepared by

Vladimir Gacesa

November, 2012

Executive Summary

HiSeis Pty Ltd acquired high resolution seismic data for Minerals and Metals Group (MMG) over the Rosebery Mine in Tasmania between the months of February and August 2012. The acquisition phase of this project included drilling holes for explosives, 2 VSP surveys and the acquisition of approximately 2.0 km² of 3D data.

HiSeis crew, accompanied by MMG, drilled a total of 1956 holes (out of a planned 1975) for the explosive sources during preparation for seismic survey. The Drilling of these source holes was completed over a time period of 4 months.

A single and static seismic patch was then executed that complied with planned designs. This had an active receiver patch of 960 channels, constructed with 10 receiver lines of 96 channels, running in an East-West orientation. 20 source lines were oriented perpendicular to receiver lines and single patch definitions included 1975 expected source points. This coverage aimed to produce adequate fold¹ required to image major subsurface target geology to a depth in excess of 1.5km.

A total of 1776 source points were acquired over the Rosebery 3D spread of a planned 1975.

Seismic information was collected using the Seistronix EX-6 seismic acquisition system, measuring micro-scale seismic responses created by explosives as a seismic source.

Final standby agreements address a total of 119.35 hours lost due to circumstances outside the control of the HiSeis. Of this time lost:

- 75.85 hours lost due to Seistronix EX6 repairs and maintenance
- 6.17 hours lost due to the pace of explosive shot firers
- 24.06 hours lost due to bad weather
- 13.27 hours lost in unclassified fields.

Overall, the acquisition of high resolution 3D seismic data was successfully completed over the prospective area, adapting an approach that accommodated the requirements of both HiSeis Pty. Ltd. and MMG Ltd.

Contents

Executive Summary.....	i
Table of Figures.....	ii
List of Tables	iii
Introduction	1
Pre-Acquisition.....	1
Overview	1
Equipment:.....	1
Vehicles:.....	1
Survey Personnel	1
HiSeis Pty Ltd.....	2
Coordinate Surveying.....	2
Acquisition	3
Overview	3
Survey Layout.....	3
3D Seismic Survey	3
Summarised Survey Statistics	7
Shots.....	7
Standby	8
Health and Safety.....	9
Recommendations for Future Surveying	9
APPENDIX A.....	A
APPENDIX B.....	B
APPENDIX C.....	H
Executive Summary.....	H
Survey Aims.....	H
Acquisition	I
Analysis of Surface Geophone Results.....	I
Analysis of VSP Results.....	L

Table of Figures

Figure 1 – Final Surveyed Coordinates.....	4
Figure 2 – Receivers and Sources (Receivers Green, Sources Red)	5
Figure 3: shot statistics over the acquisition phase of the project.....	7

Figure 4 - Shot rate statistics.....	7
Figure 5 - Distribution of standby time	8
Figure 6: Fig 1. D booster on the left and power-gel on the right. Power gel much better than D booster, but runs out of energy by 600-700m offsets. Not really good enough.....	B
Figure 7: Fig 2. D booster on the left and power-gel on the right. Same result as previous: Power gel much better than D booster, but runs out of energy by 600-700m offsets. Not really good enough. I would recommend a larger charge to achieve good energy over 1000m or more of offsets.....	C
Figure 8: In this example of Power gel spectrum the energy is only strong in the 10-90 Hz band, which is not very good. Despite having barely acceptable energy, the frequency content is not really acceptable for a small explosive well coupled to rock.	D
Figure 9: D booster spectrum. Good energy to approx 120 Hz. Not particularly good for a small explosive. We would hope to have up to 150-200 Hz in a good hole. Note that good energy 10-100 Hz considered necessary for reasonable resolution of target. D booster is unacceptable in terms of both spectrum and energy.....	E
Figure 10: Power gel spectrum. Most energy is in the 10-120 Hz band in this example. This is acceptable, but not a great result for an explosive source in rock. Better than a weight drop spectrum though. On balance acceptable.	F
Figure 11: Spectrum of 60 g booster done in Nov 2011. Good energy to about 120=140 Hz. Quite variable vs position of geophone. This may be due better rock/coupling or explosive type. Boosters usually provide better frequency content due to greater velocity of detonation.	G
Figure 12: Examples of shot records with VSP string at various depths plus one panel with surface geophones (second last from right). Most of the energy is in tube waves, which appear as diagonal bands of signals.....	I
Figure 13: Surface geophone response to 60g of explosive 50-350m from shot-point. The refractions, a proxy measure of returned signal strength, are relatively strong; until the geophones that are placed into mossy and humus rich soil near the top of the hill ridge.....	J
Figure 14: Combined VSP and surface records with VSP tool at maximum depth. The VSP data is the left portion of the panel (that has tube wave chevron patterns) and the surface geophones are the right portion. The record on the left (FFID=1232) used a “horizontal” hole and the record (FFID=1233) on the right used a “vertical” hole. Both used a single 75 g booster. Note the raindrop noise, random spikes, on the uncovered geophones.	K
Figure 15: Zero offset VSP with string top set at 50m, lowest sensor at 280m (rightmost). The first energy is relatively clear in the high gain presentation of the data, the first blue pulse. Also, there is a major fracture at approximately 210-220m in the hole. Such fractures are sources of tube wave emission when the p-wave arrives at the fracture location.	L
Figure 16: First two string positions, 50, 250, 450m to top sensor. Ideally there should be low noise prior to received energy (a white clear zone in the upper portion of the plots as in the left-most panel) The rightmost panel also has noise from a nearby drill starting up.	M

List of Tables

Table 1 - HiSeis Staffing.....	2
Table 2 - Final survey parameters.....	6

Introduction

This final acquisition report is divided into five main sections: the Executive Summary (above), this Introduction, Pre-Acquisition, Acquisition and Recommendations for Future Surveys. Each section outlines specific data, summaries and explanations relating to all aspects of the seismic acquisition in the Mount Black prospect area, Rosebery, Tasmania.

Pre-Acquisition

Overview

The Pre-Acquisition phase includes all in-field equipment deployment and survey preparation time prior to the physical collection of seismic data. The Pre-Acquisition survey phase began on the 6th of February 2012 with the arrival of HiSeis field crew and was continued until the first day of data acquisition on the 19th of June.

HiSeis crew was drilling source holes (for explosives) from the 6th of February to 19th of June. Rugged terrain and very limited access for vehicles made this job extremely challenging for the crew. In total, 1776 holes (1.2m deep and 40mm wide) were drilled from 1975 source points.

Equipment:

Acquisition equipment was stored at the exploration office in Rosebery and the laydown area at Mount Black for the duration of the survey to allow for easy access to the crew during the acquisition phase.

Transport for the VSP winch from mine site to logging site on Mount Black was organized by MMG.

Vehicles:

HiSeis field crew operated three mine-spec utility vehicles as a means of transport and in-field operations. These vehicles were sourced from MMG. Furthermore, HiSeis crew hired a minivan from local Burnie rental dealer that was later returned to the same depot.

MMG provided a metal shed for on-site recording office (dog box) for acquisition, which was located on Mount Black to the Eastern extents of the seismic spread. Mobile generators were provided to power the dog box and any electronics requiring uninterrupted power.

Survey Personnel

The survey personnel consisted of HiSeis staff (drilling crew, line crew and geophysicists), MMG personnel (line cutters and field help) and Mancala (shot firers). Coordinate surveying was done by PDA surveying (organized by MMG).

Personnel	Position
Luke Gibson	Field Operations Manager
Anton Kepic	Technical Director
Vladimir Gacesa	Geophysicist
Jai Kinkela	Geophysicist
Robert Martin	Geophysicist
Ralph Lyster	Drilling Supervisor
Padhraig Guthrie	Line Crew
Robert Cunningham	Line Crew
Lucy Shell	Line Crew
David Williams	Line Crew
Andrew Lawson	Technician

Table 1 - HiSeis Staffing

Coordinate Surveying

Line marking and clearing was organized by MMG. Coordinate surveying and stakeout was undertaken by MMG and HiSeis staff prior to the commencement of drilling. PDA staff were involved in the surveying throughout the data acquisition period.

A precise location for shot and receiver pegs is required in order to produce accurate seismic data. Due to the access/terrain conditions throughout the survey area, GPS positioning was unable to achieve the required precision. Hence, 'total station' coordinate surveying was required and this was coordinated by PDA.

Acquisition

Overview

Acquisition refers to the physical collection of seismic measurements through the production of seismic waves from the explosive source (shooting) at various locations throughout the survey area. These manufactured waveforms are then measured by the active geophone array (live patch).

Shooting started when the entire geophone patch was laid out, connected, powered-up, error-checked and ready to record data. Due to there being a single live patch, daily acquisition was planned based on line accessibility, weather and radio coverage. During acquisition, radio repeaters were moved a number of times to ensure adequate radio coverage for both triggering and communications.

Shooting was carried out continuously (7 days a week) for the duration of the survey, typically between the hours of 7:30am to 4:00pm each day. Weather conditions were typically favorable with some rain and strong winds at the beginning of survey.

During periods with rain and wind, data quality (signal to noise) was monitored within the acquisition software. General agreement was to stop shooting if the signal to noise was under an acceptable level (67%).

Accessibility and terrain issues resulted in the use of explosives as a source of seismic energy. After testing, it was found that 1-2 120g Pentax G boosters provided adequate energy for measurable signal across the entire spread length of the spread.

Survey Layout

3D Seismic Survey

The survey plan was comprised of a single patch with 10 receiver lines and 20 sources lines.

The survey plan was to collect data across 10 receiver lines of 96 channels, totaling a live channel count of 960 for the active and static patch. Receiver positions in the orientation of the receiver lines (in-line) aimed to be equidistantly spaced at intervals of 10m. Distance between sequential receiver lines (x-line) was set to 100m.

Source point distribution was designed to incorporate 20 source lines. In-line intervals of 10m were used for source points outside of the active receiver patch, and intervals of 20m through the center of the patch. X-line intervals of 80m were used over the entire survey. Line length was 1.24km with lines 1,2,18,19 and 20 having 125 source points (10m spacing) and 15 lines with 90 source points (10m and 20m spacing)

Comparison between planned source and receiver locations and final surveyed points can be seen below in **figures 1 and 2**. Nominal survey parameters can be seen in **Table 2**.

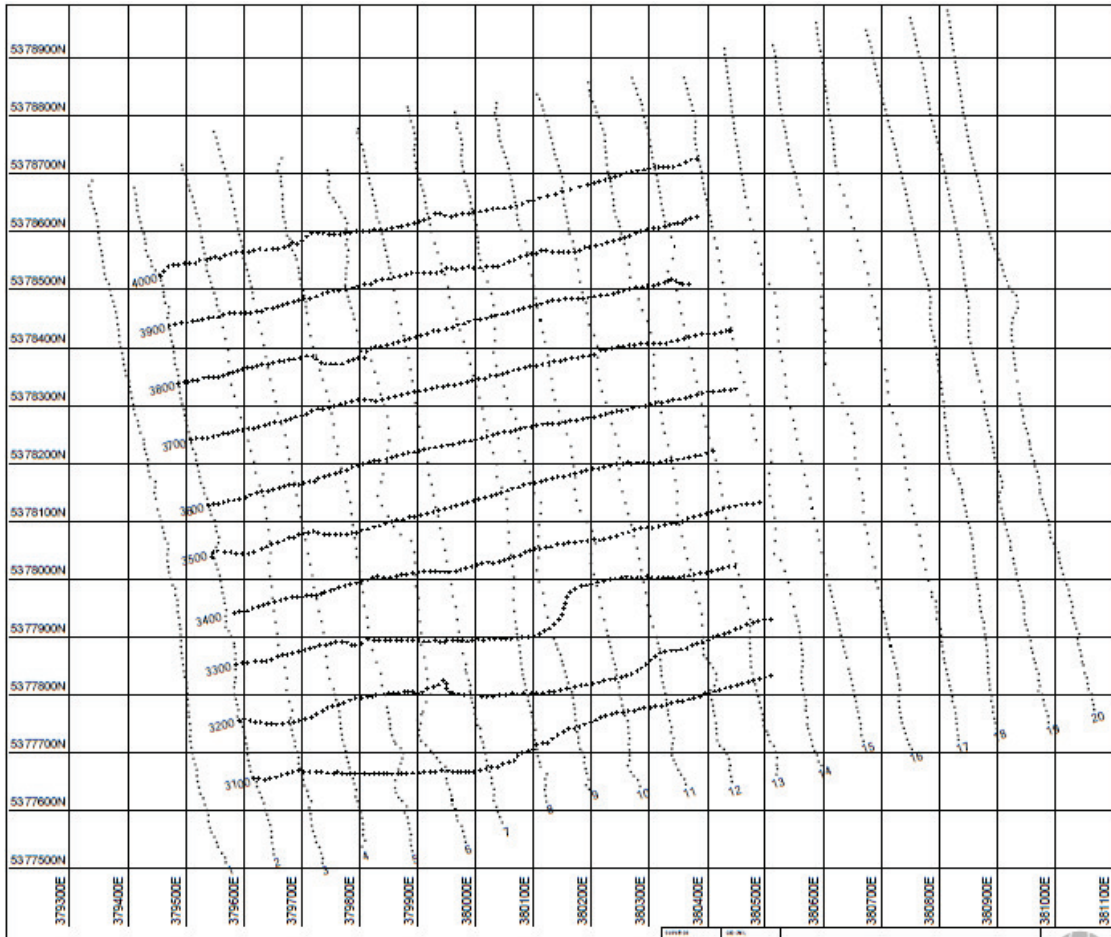


Figure 1 – Final Surveyed Coordinates



Figure 2 – Receivers and Sources (Receivers Green, Sources Red)

Parameter	Final
Total Acquisition Area	~2.0 km ²
Number of Receiver Lines	10
Live Channels/Patch (Nominal)	960
Live Channels/Receiver Line	96
Receiver Interval (In-line)	10m
Receiver Interval (X-line)	100m
Nominal Receiver Density	1111.1 per km ²
Total Unique Source Locations	1776
Nominal Shot Point Density	397.2 per km ²
Number of Source Lines	20
Source Interval (In-line)	10 & 20m
Source Interval (X-line)	80m
Record Length	3 s
Sample Rate	2ms
Source Type	Explosives (1-2 x 120g Pentax G booster)

Table 2 - Final survey parameters

Summarised Survey Statistics

Shots

A total of 1776 effective shots were collected, 129 shots misfired and 70 stations abandoned over the 1975 unique shot locations throughout the 3D seismic spread. These were collected over a total of 44 shooting days. This yields an average of 40.3 shots per day for the duration of data collection (first shot fired to last shot fired).

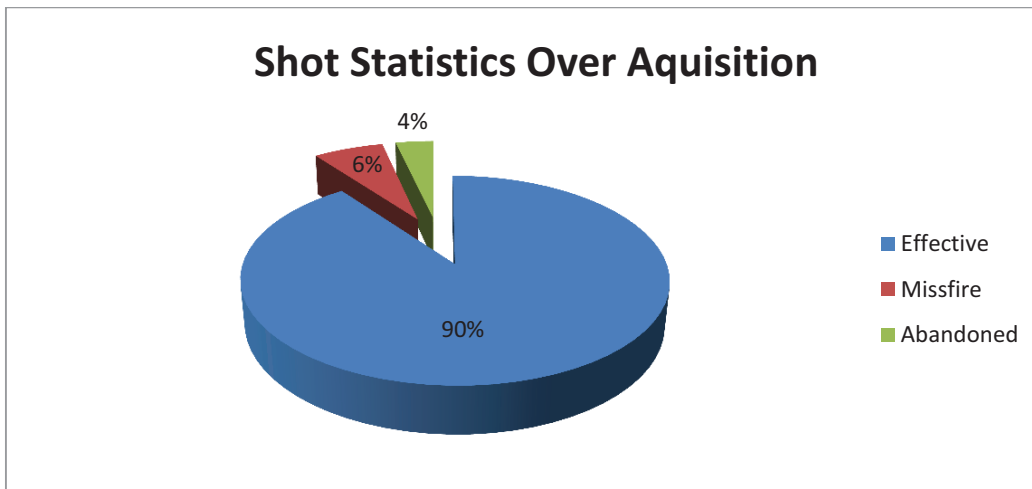


Figure 3: shot statistics over the acquisition phase of the project

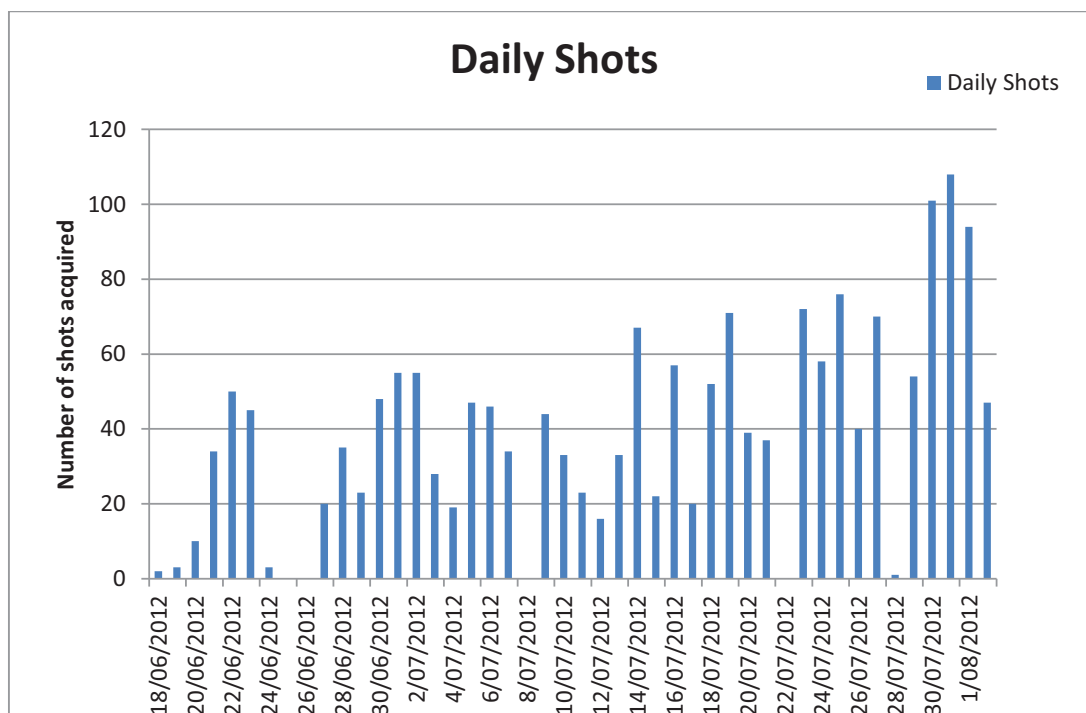


Figure 4 - Shot rate statistics

Standby

Based on contractual arrangements, stand-by charges were incurred following the readiness of all survey equipment and personnel at the project site required for the project to operate, where factors outside of HiSeis control inhibited production. Standby time includes:

- Working time lost due to wet, extreme cold or otherwise adverse weather conditions including wind, excessive snow;
- Delays or extra time spent as a result of any act, default, direction, instruction or request of the company or company's Representative, including time waiting on company's direction. This includes reprioritizing the acquisition sequence;
- Daily and weekly Safety Meetings called by the client;
- Time lost due to access restrictions or permitting problems beyond the control of the contractor;
- Time lost due to vandalism, theft, or malicious damage to seismic equipment by any party;
- Crew safety and Inductions as required;
- Geophone, Cable leakage tests as required by the company prior to or following survey commencement;
- Delays, wash downs, inspections due to any compliance requirements of local and federal government laws and regulations;
- Delays due to Local Management, Local Government or Government Traffic Management or Indigenous Persons requirements;
- Crew safety meetings and inductions as required by the Client

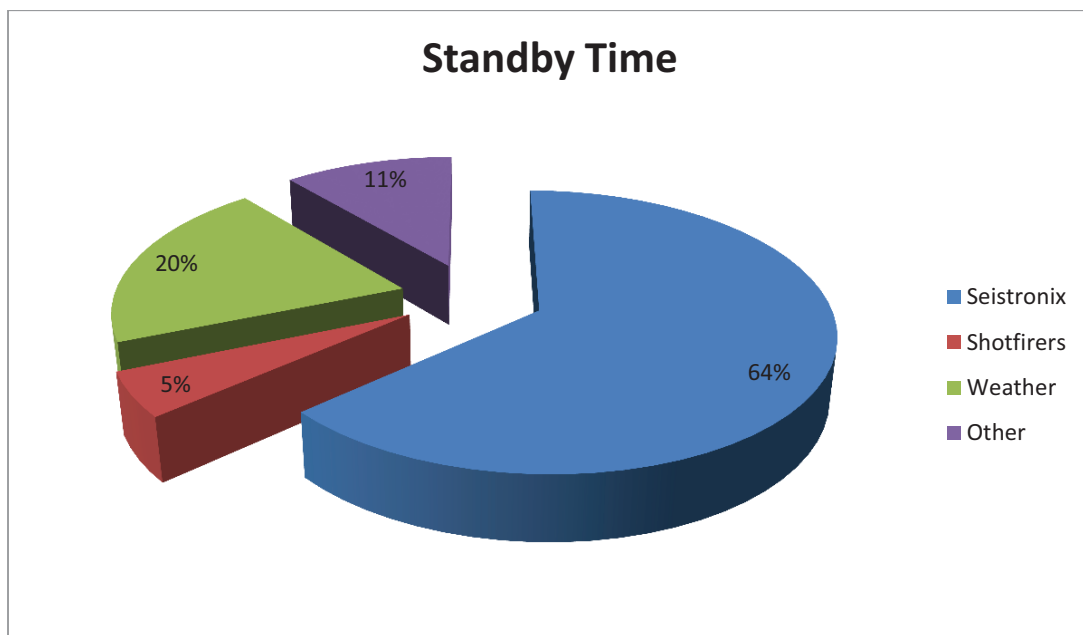


Figure 5 - Distribution of standby time

Health and Safety

Only one safety incident was reported. A very brief summary is provided. Please see appendix D for more details.

Incident: Car was damaged on access road and oil leaked on track.

Resolution: Adjust speed to condition on track, and use vehicle with high ground clearance.

Recommendations for Future Surveying

Several recommendations can be made for future application of seismic surveying in the Mount Black area. These recommendations aim to maximize productivity, minimize environmental impact, increase the quality of geophysical data, increase the safety of the operation, reduce loss of time and reduce the risk of equipment damages and loss.

These recommendations include:

- In field communications:
 - Many of the problems associated with efficiency of shooting and the misfire of shots was a result of bad radio reception. Had the repeater been set up correctly from the beginning, this would have resolved both the above issues.
- Land access and environmental sensitivity:
 - The terrain conditions faced throughout the survey proved to be very challenging. There was minimal vehicle access and the cut tracks along planned lines through the forest were steep and dangerous. Access to areas of the spread could take up to 1 hour. Given the circumstances, there is little that either party could have done to mitigate this issue.
- Timing (weather):
 - Acquisition was planned to be conducted over the dry summer/autumn months. Due to the issues associated with drilling the source holes, most of the acquisition was done in the unfavourable weather conditions of winter with wind and rain. This also had negative impacts on safety. To overcome this, forward planning of the time taken to do the different tasks associated with acquisition is crucial. This will allow more efficient acquisition of data, and a resultant lower overall cost.
- Acquisition:
 - Dual source crews would increase production rates, especially due to the time taken to move from one source location to the next.
 - Dual drilling crews in order to finish the drilling in an acceptable time frame would allow acquisition of shots in favourable weather conditions (summer).

- Having water (for explosive coupling) placed in strategic locations throughout the spread to reduce time of water transportation
- Vehicles:
 - Using only vehicles with high ground clearance.
 - Keeping to indicated speeds in the vehicles.
- Drilling:
 - Increased air pressure for air drill – after implemented, productivity greatly increased
 - Having poly pipe for air transport already laid out prior to the drill coming through would increase drilling efficiency.

APPENDIX A

All daily field reports are provided electronically.

APPENDIX B

Explosive Test Report (A.Kepic).

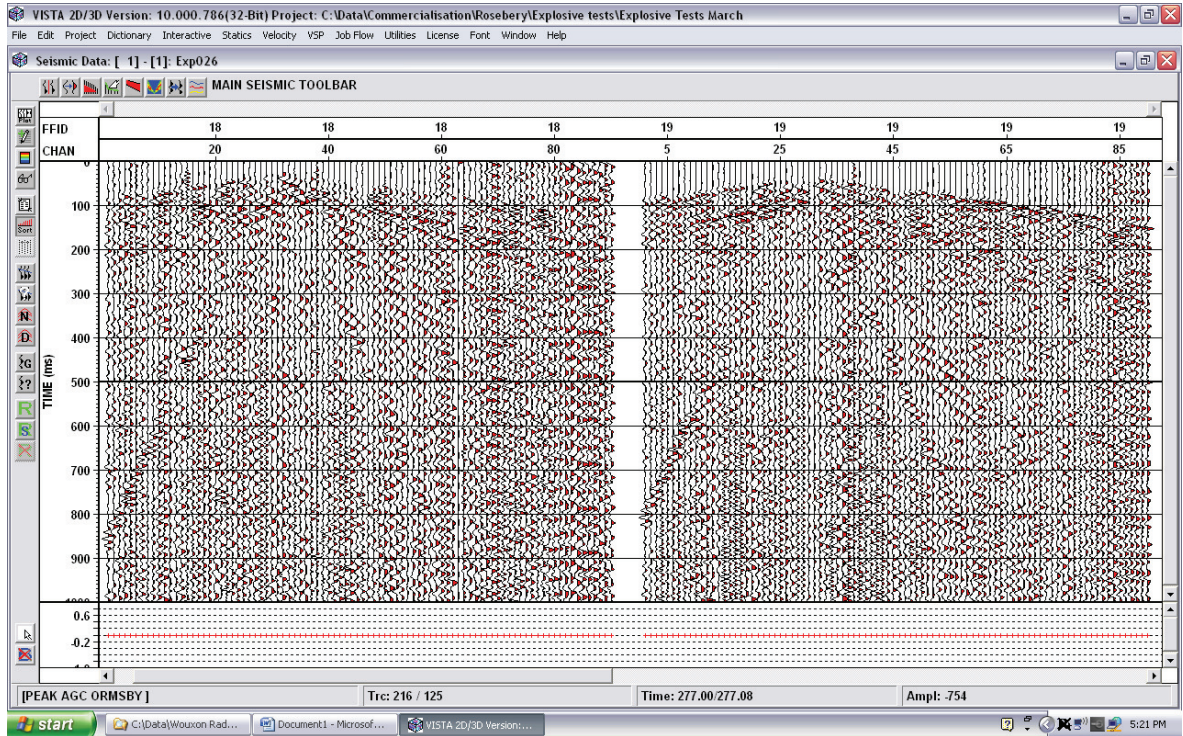


Figure 6: Fig 1. D booster on the left and power-gel on the right. Power gel much better than D booster, but runs out of energy by 600-700m offsets. Not really good enough.

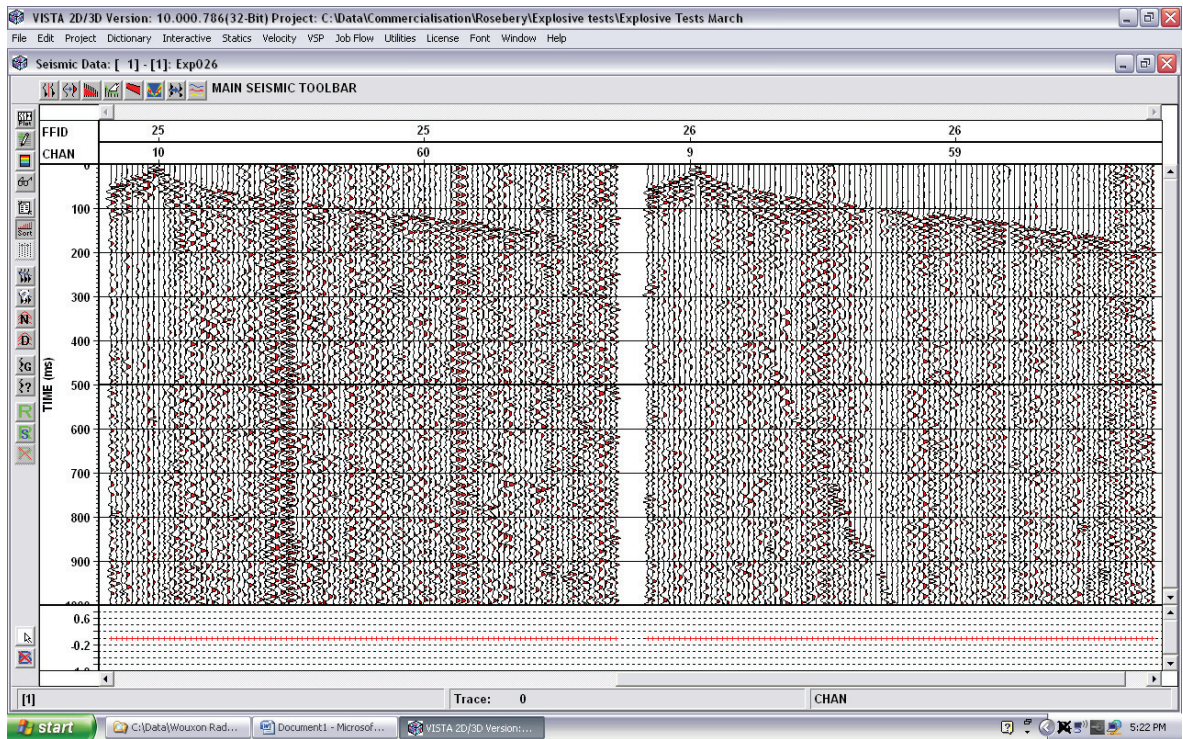


Figure 7: Fig 2. D booster on the left and power-gel on the right. Same result as previous: Power gel much better than D booster, but runs out of energy by 600-700m offsets. Not really good enough. I would recommend a larger charge to achieve good energy over 1000m or more of offsets.

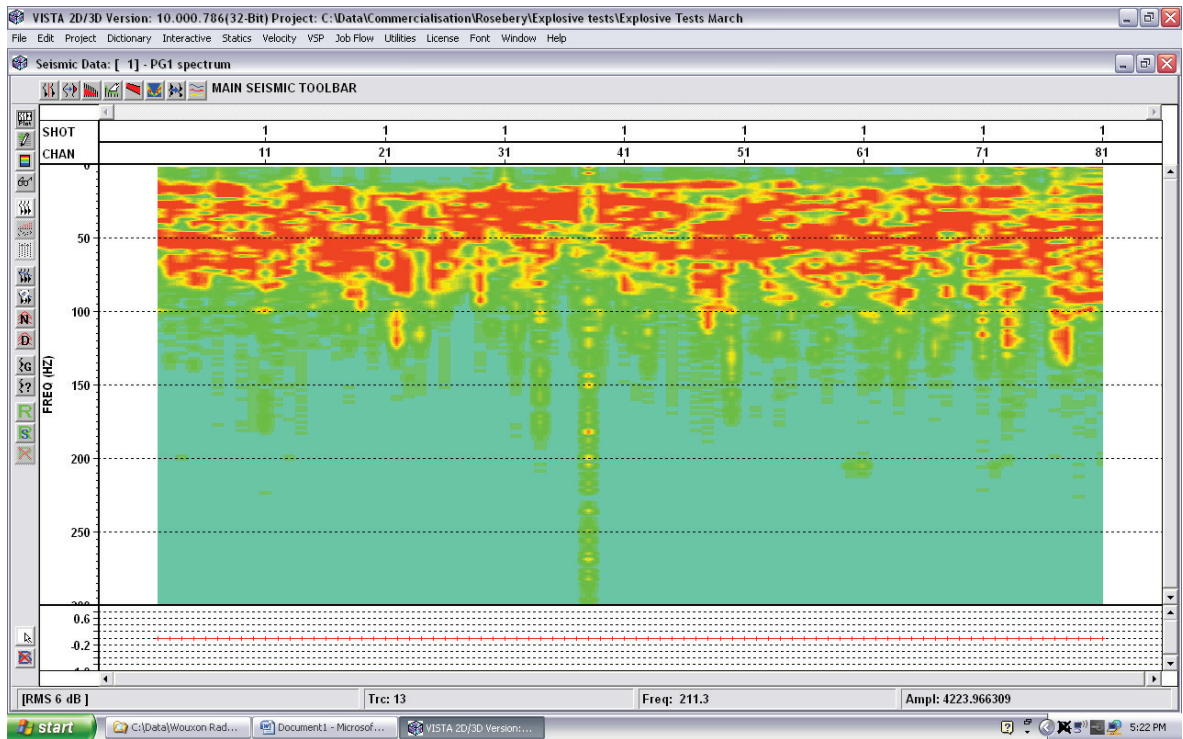


Figure 8: In this example of Power gel spectrum the energy is only strong in the 10-90 Hz band, which is not very good. Despite having barely acceptable energy, the frequency content is not really acceptable for a small explosive well coupled to rock.

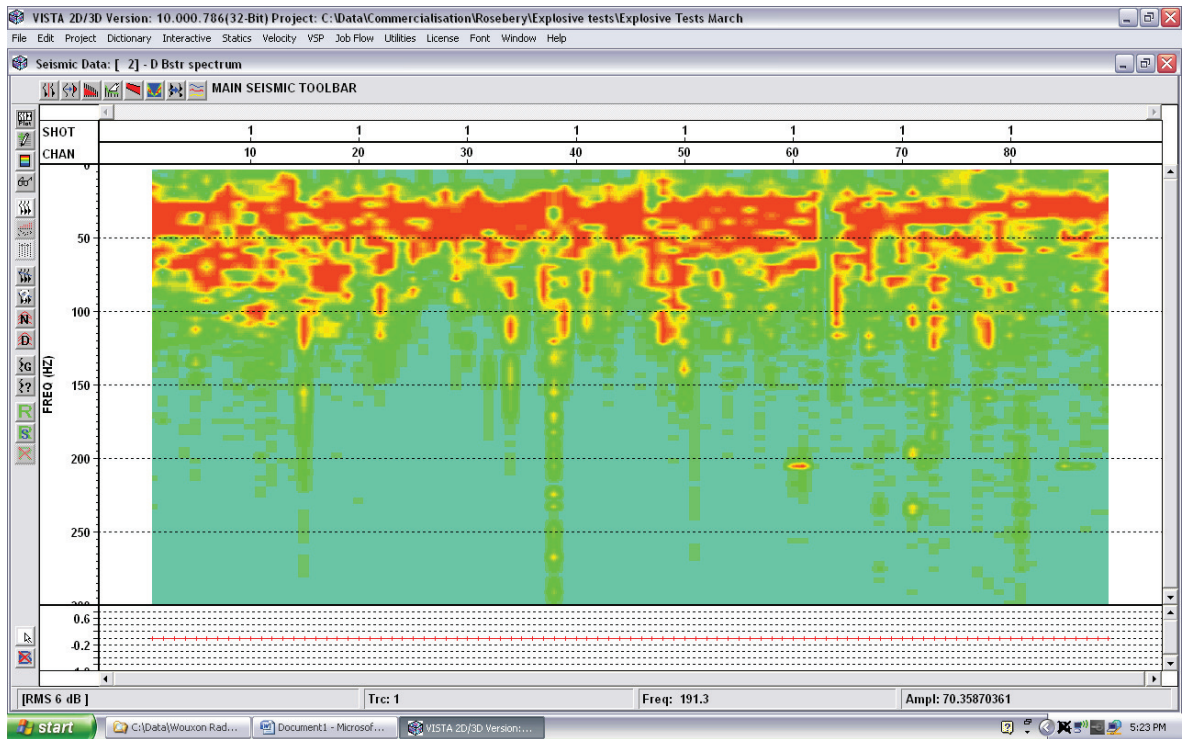


Figure 9: D booster spectrum. Good energy to approx. 120 Hz. Not particularly good for a small explosive. We would hope to have up to 150-200 Hz in a good hole. Note that good energy 10-100 Hz considered necessary for reasonable resolution of target. D booster is unacceptable in terms of both spectrum and energy.

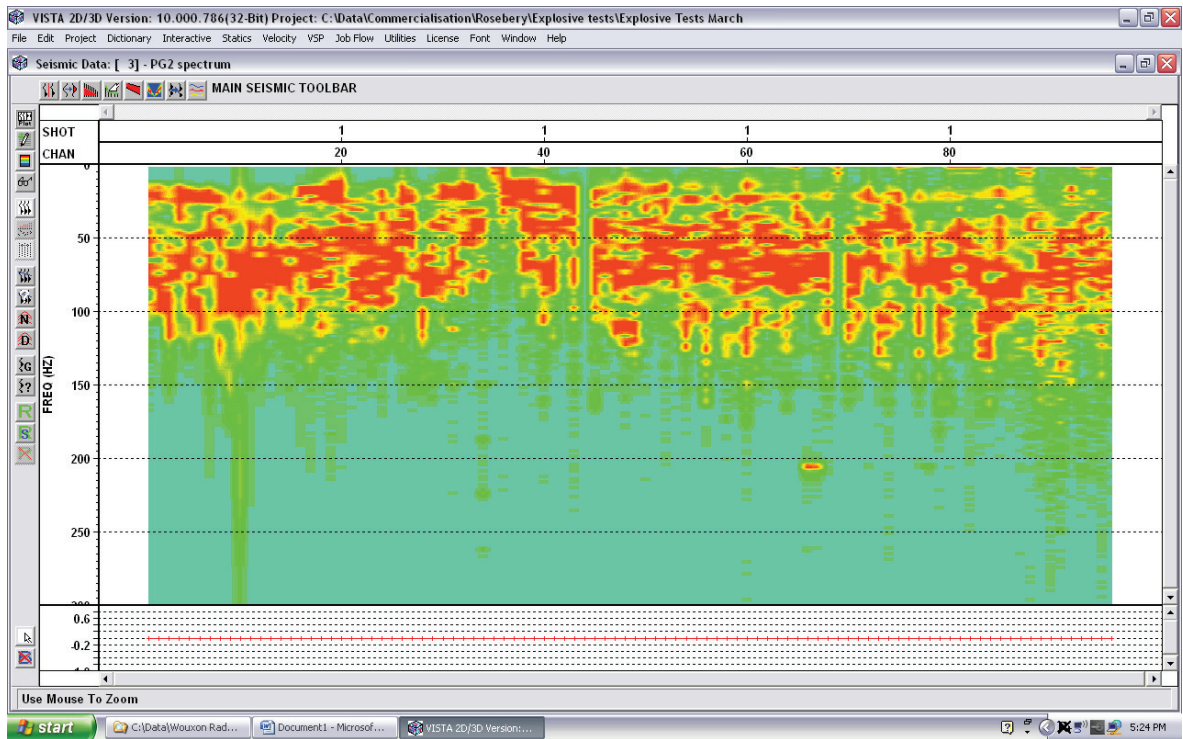


Figure 10: Power gel spectrum. Most energy is in the 10-120 Hz band in this example. This is acceptable, but not a great result for an explosive source in rock. Better than a weight drop spectrum though. On balance acceptable.

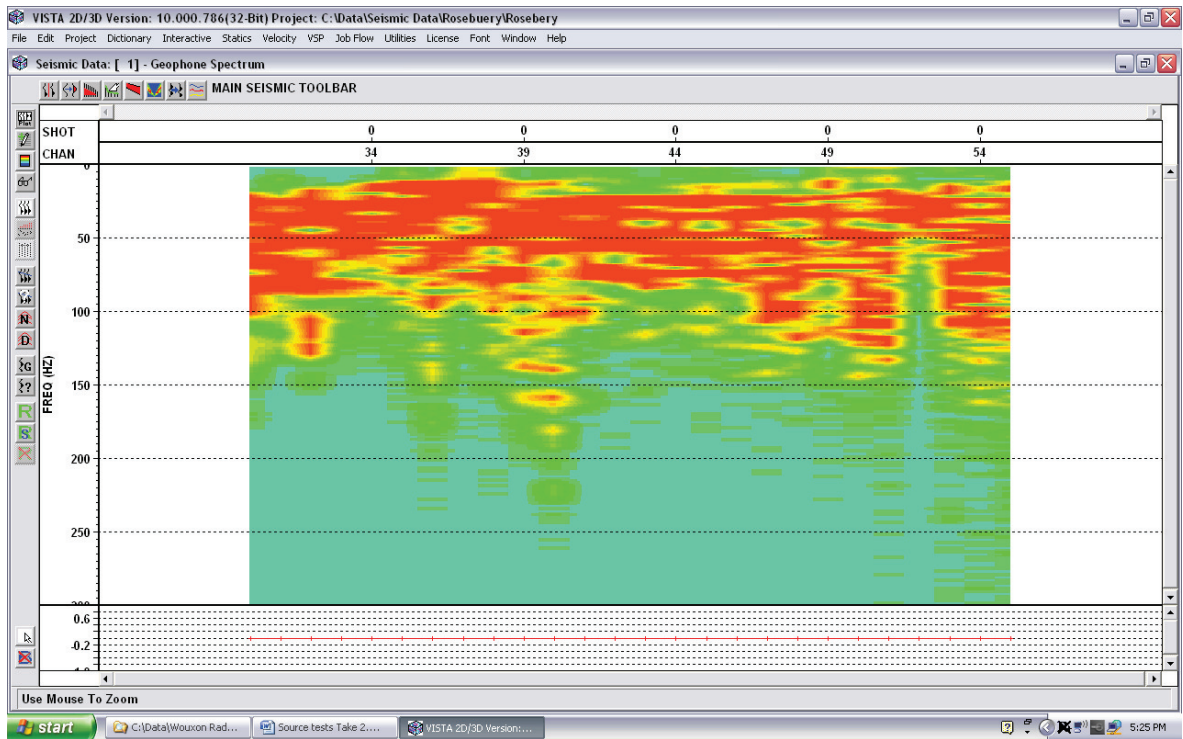


Figure 11: Spectrum of 60 g booster done in Nov 2011. Good energy to about 120=140 Hz. Quite variable vs. position of geophone. This may be due better rock/coupling or explosive type. Boosters usually provide better frequency content due to greater velocity of detonation.

APPENDIX C

VSP Test Report (A.Kepic).

Executive Summary

Explosive source testing demonstrated that small explosive charges in fairly shallow holes should deliver reasonable energy to geophone sensors about 1 km or more away. The charge sizes were generally 60-90g of PETN in a 1200 mm hole. In these tests a well coupled geophone could clearly detect first arrival seismic waves approximately 100-700m from the shot. All test shots, some with up to 120g of explosive, were well contained in a 1200-1500 mm hole, with no fly-rock or craters.

The coupling of energy to the ground while adequate was not as good as hoped. Most test holes did not reach fresh rock and insufficient water was contained in the hole to couple the energy efficiently to the rock-mass. Thus, holes should try to reach very competent rock and charge sizes to 150g can be used without significant fly-rock. A single cast booster/explosive of 100-150g in a deeper hole of 1500 mm is recommended.

The geophones should be planted in the weathered rock where possible. Soil, moss and humus cover should be avoided as the geophones planted in this material are clearly less sensitive. Also, the wet and rainy weather of the area near Rosebery means that raindrop noise may be problematic. Thus, the geophones should have some loose soil humus cover where possible to attenuate these noisy events.

A zero-offset vertical seismic profile (VSP) survey failed to provide the desired velocity with depth profile because the direct waves were either too weak to be detected, or the sources of noise too strong. The hydrophone string appeared to be fully functional and was deployed with no significant issues, but the relative strength of direct arrivals vs ambient noise is too low to pick the early, direct arrivals. Noise from a nearby drill rig and the mine appear to be significant problems. Tube waves in the hole were found to propagate without much loss; thus, the trapped noise energy masks the relatively weak direct waves. Another aspect that may have lowered signal-to-noise is the possibility that a nearby fault or dyke close to the shot-holes may have scattered the energy away from the borehole.

If a velocity profile is needed then the VSP survey should be re-trialed with tube-wave baffles (a new development) in place to increase signal-to-noise. Also, a repeatable impact source that can be easily positioned along road/track would allow testing for better positioning of the source.

Survey Aims

The principal aim was to test the viability of a small explosive source for imaging the Rosebery area geology. This would be achieved by recording the post-blast ground waves with geophones on the ground and a hydrophone array in a newly drilled borehole. Good signal-to-noise on the geophone array would indicate the source will perform acceptably. A secondary aim would be to gather time-depth conversion. Such data is useful for processing and interpretation later. Also, the hydrophone array data will also further indicate how much energy reaches the target.

Acquisition

The data was collected in a single day, Thursday 10 Nov 2011, starting at approximately 11am after equipment set-up and testing. Detonator and trigger tests were performed the previous day. Firstly, tests with a detonator and several nearby geophones verified the trigger was operating correctly. Then noise, with a surface impact, of the VSP array was analysed to verify that it was electrically correct. The VSP tool was lowered by 200m increments with 4 elements of overlap between “drops” of the array. The array was allowed time, about 5-10m, to settle with respect to hydrostatic pressure.

The first record was taken with the hydrophone array at 50m (top sensor element position), then deployed at 250, 450, 650, 850, 1050, and lastly 1230 to avoid hole bottom at about 1470 for the lowest sensor. At a depth of 850m extra channels were added (30ch) of surface geophones that headed up-hill with 10m spacing between geophones. As the VSP hydrophones and surface geophones were combined into a single record with the recording system there are 5 unconnected channels (1-3 and 28-29) due to link to computer and a small cliff face at the start of the geophone line.

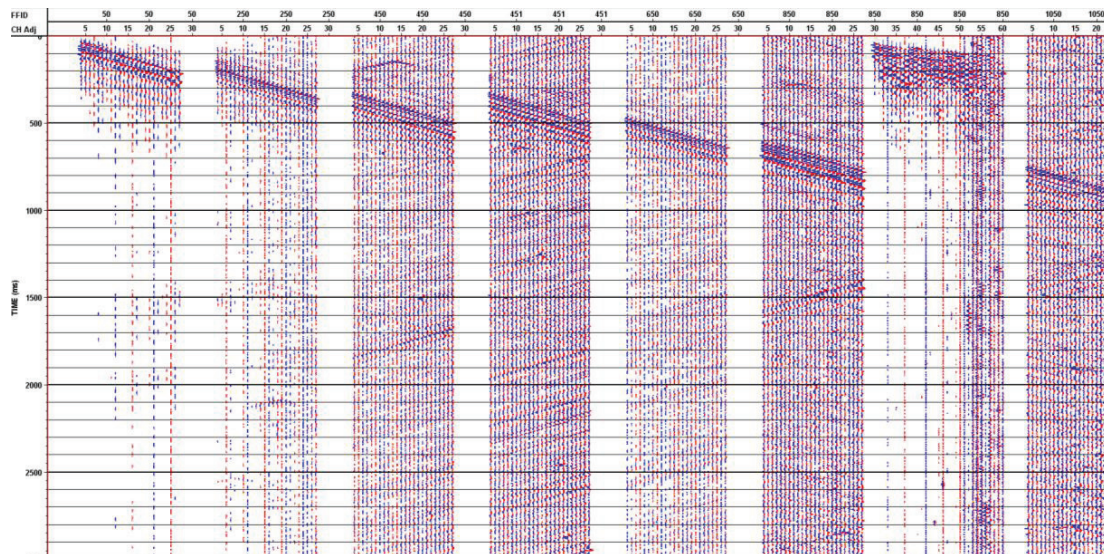


Figure 12: Examples of shot records with VSP string at various depths plus one panel with surface geophones (second last from right). Most of the energy is in tube waves, which appear as diagonal bands of signals.

After several shots it became apparent that there was insufficient signal-to-noise in the VSP hydrophone string to obtain good first break data. Firstly, it was discovered that a nearby drilling rig was the cause of most of the noise (see third panel in Figure 12)

Analysis of Surface Geophone Results

In general, the small explosive charges provided reasonable (refraction) signals except for a group of geophones that were planted in soil humus at the distant end of the geophone line (Figure 13). The signal vs background noise ratio is 10:1 to 5:1 for geophones up to 300m away on shots near the VSP area. Data from the single shot placed about 400m further down-slope were of similar quality. Thus, the fresh rock does not seem to attenuate the signals very much. It should be noted that “raindrop noise” is prevalent in many of the records (random noise spikes occurring during rain periods, see Figure 13).

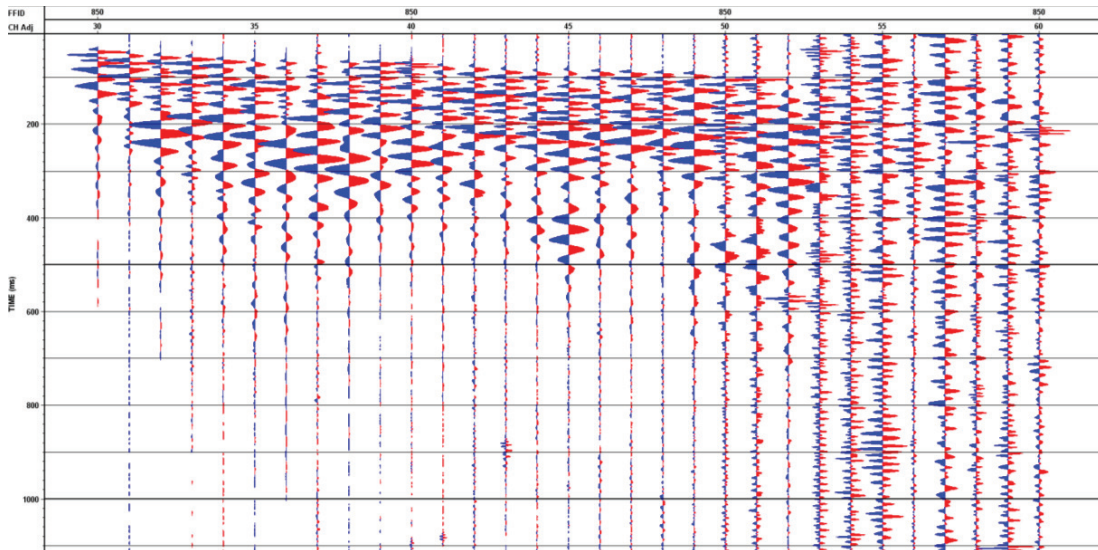


Figure 13: Surface geophone response to 60g of explosive 50-350m from shot-point. The refractions, a proxy measure of returned signal strength, are relatively strong; until the geophones that are placed into mossy and humus rich soil near the top of the hill ridge.

Many of the shots in the VSP tests were inconsistent in explosive coupling. This was noted in the relative strength of refractions and tube waves in the VSP data. Many holes did not allow water to remain with the explosive package because they were drilled slightly upward – a more comfortable position for the drillers (Figure 13 for example). Also, the use of multiple small boosters tied together did not seem to perform as well as expected. Single charges weight-for-weight performed better (Figure 14).

The greatest influences on received signal strengths are the coupling of explosive to rock (the quality of hole and water coupling) and the way the geophones are planted in the ground.

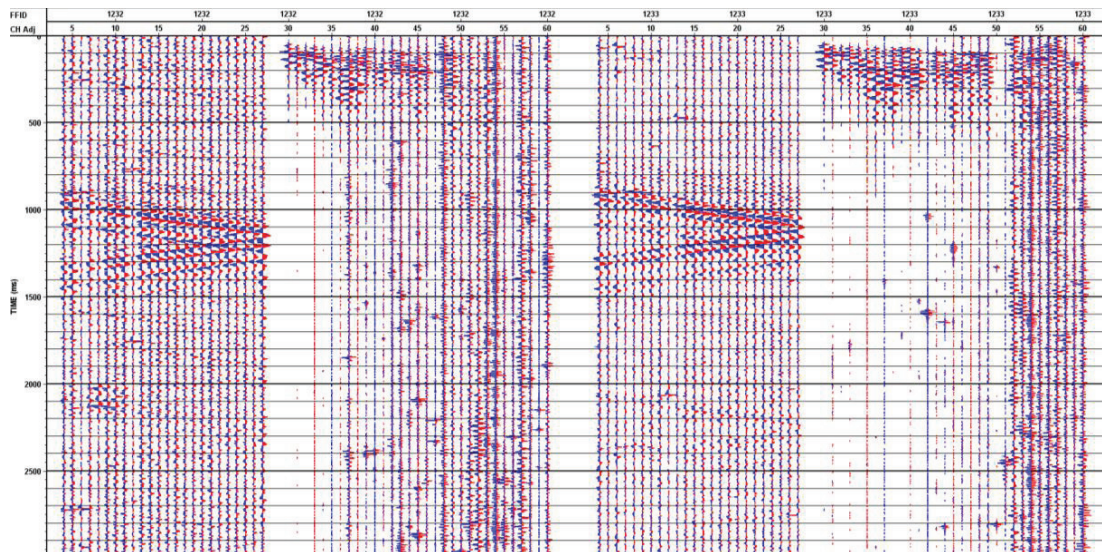


Figure 14: Combined VSP and surface records with VSP tool at maximum depth. The VSP data is the left portion of the panel (that has tube wave chevron patterns) and the surface geophones are the right portion. The record on the left (FFID=1232) used a “horizontal” hole and the record (FFID=1233) on the right used a “vertical” hole. Both used a single 75 g booster. Note the raindrop noise, random spikes, on the uncovered geophones.

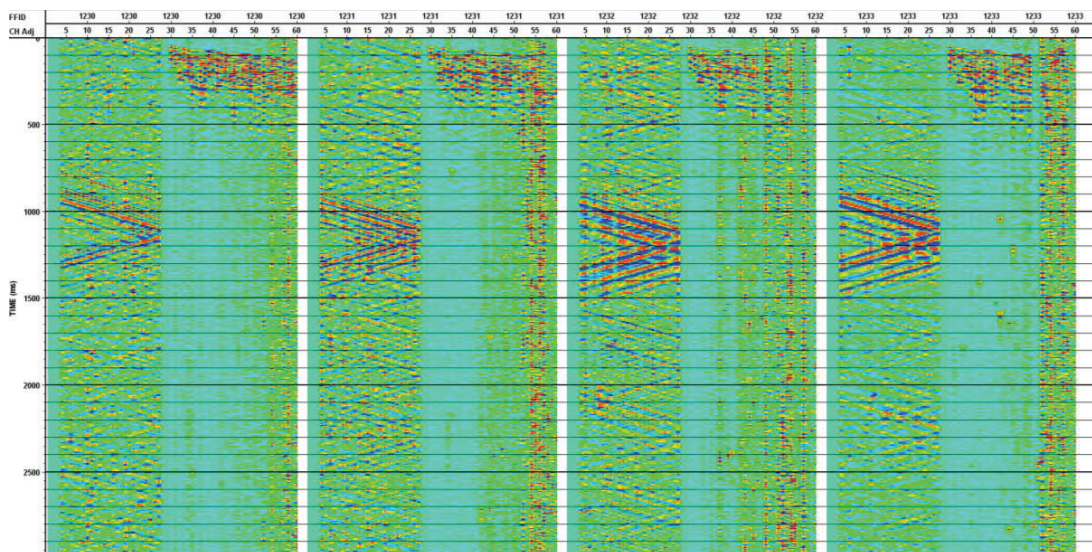


Figure 14: Four repeat shots with different holes and explosive strengths. From left to right the shots were with 3x30g, 4x30g hole re-used, 1x75g in reused hole, and 1x75g in new hole. The use of multiple boosters tied together does not perform as well as a single but smaller explosive in a good hole.

Analysis of VSP Results

The VSP data is relatively weak. The tube waves appear clearly at depths up to about 800m, and then become somewhat weak as well. These organ-pipe like modes have a characteristic slope and form diagonal bands in the data. Apart from the first 200m there is insufficient quality of data to prove velocity information. The velocities in the top 200 or so m appear to be of the order of 4500-5000m/s (4700 m/s average), which is unsurprising for a crystalline rock environment.

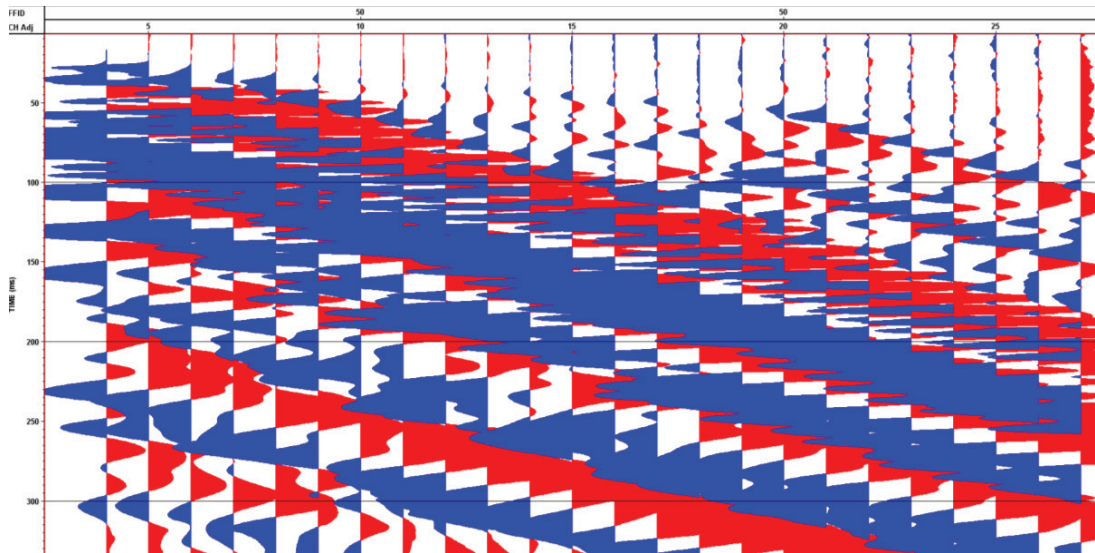


Figure 15: Zero offset VSP with string top set at 50m, lowest sensor at 280m (rightmost). The first energy is relatively clear in the high gain presentation of the data, the first blue pulse. Also, there is a major fracture at approximately 210-220m in the hole. Such fractures are sources of tube wave emission when the p-wave arrives at the fracture location.

The data appears to have low signal-to noise. It is not clear whether the hydrophone array was in some way not providing good signal because of electric malfunction – unlikely as the tube wave signals have good fidelity, but not great S/N either. P wave energy from the explosives were not strong. However, the surface geophones have reasonable signal-to-noise when well coupled. Thus, there appears to be trapped tube-wave energy from nearby drilling or mine activity. This energy can be seen in the bands of tube arrivals which are often stronger going upwards (downwards – a line of energy trending downwards from left to right vs upwards – trending upwards from left to right). This can be seen in figures 16 and 17, where there are upward moving bands throughout the data. Tube-wave reflections from the top and bottom of hole are apparent (and seen from the explosion generated band of energy which bounces back and forth too). Despite turning off the nearby drill the later shots are also full of these un-damped wave-modes.

The background noise can be better handled if the tube-wave noise were better damped in the hole. Signal processing is unlikely by itself to remove these noise patterns in the data.

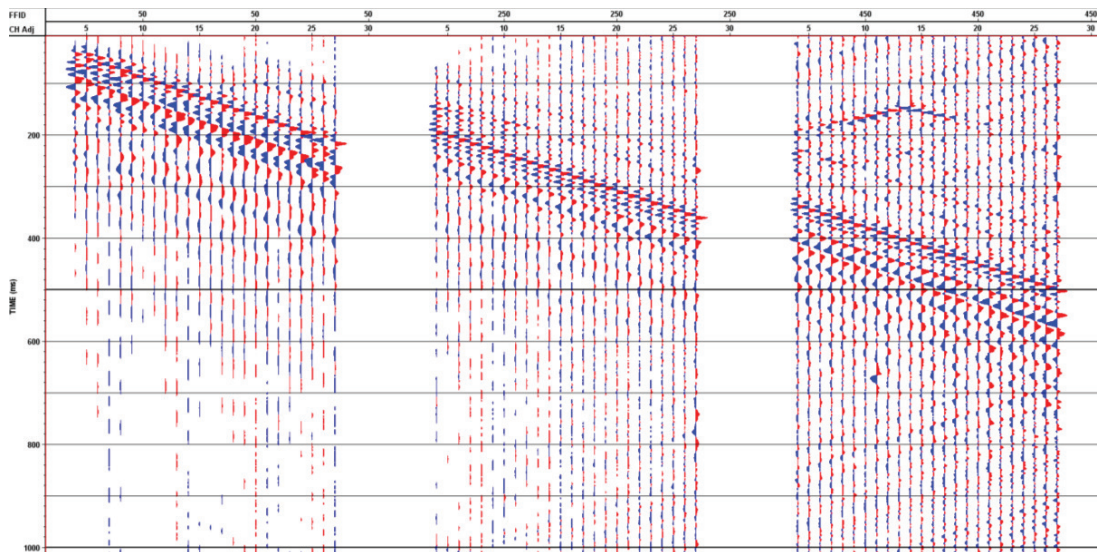


Figure 16: First two string positions, 50, 250, 450m to top sensor. Ideally there should be low noise prior to received energy (a white clear zone in the upper portion of the plots as in the left-most panel) The rightmost panel also has noise from a nearby drill starting up.

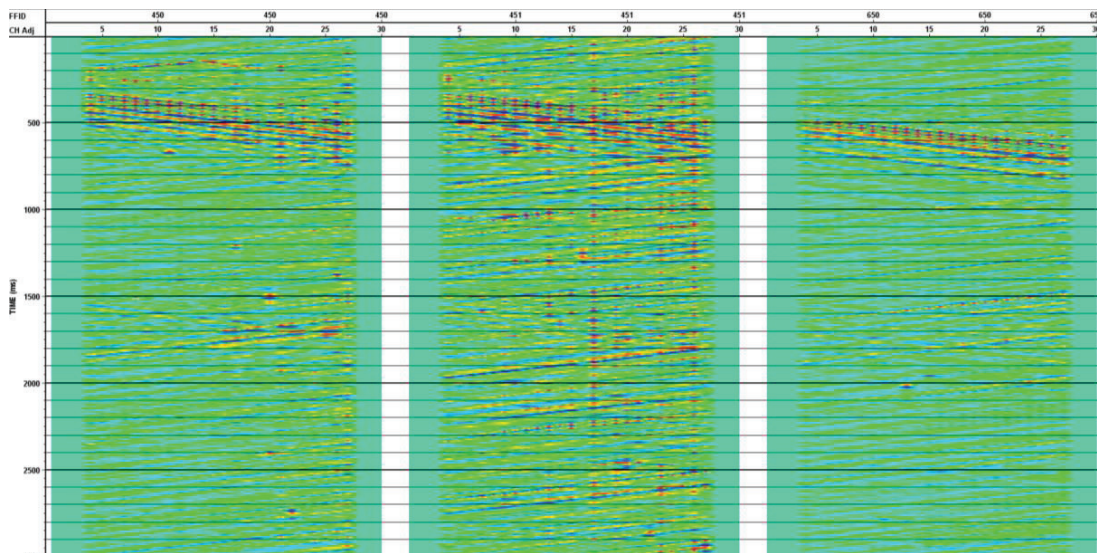


Figure 17: Examples of upward tube waves from external sources. The main down trending energy is from the explosive. However, there are many bands prior to the explosive energy arriving and much later, indicating various external noise sources.

APPENDIX C: HISEIS PROCESSING REPORT

HiSeis Pty Ltd.
Suite 4, Enterprise Unit 3
9 De Laeter Way
Bentley WA 6102
Australia



Interpretation Report

Rosebery High Resolution 3D Seismic Survey

Rosebery, Tasmania

For

Minerals and Metals Group Limited.

Report number:MMG-3DROSEINTERP12

Prepared by

Jai Kinkela

April 2013

Executive Summary

An interpretation of high resolution three-dimensional (3D) seismic reflection data collected by HiSeis at the Rosebery minesite was conducted in order to achieve a number of objectives. These were namely:

1. Determine whether the seismic method was successful in imaging geology known to exist in the area.
2. Observe whether the mineralization was being directly detected by seismic in the form of amplitude anomalies.
3. Decide whether seismic was successfully imaging target geology further down dip.

Paradigm's GOCAD was the primary software employed for the integration of a number of geophysical and geological datasets. Upon interrogating the seismic it was found that the 3DPSTM AGC cube was best suited to carrying a structural interpretation of the subsurface geology in conjunction with the instantaneous phase attribute. Utilising these two datasets allowed for the interpretation of what appears to be the Rosebery and Mount Black Faults, which were identified based on the intersection and truncation of reflector geometries.

An amplitude-consistent cube was also utilized for the purpose of direct detection of mineralization. Based on physical rock property measurements it is expected that mineralization would provide one of the largest acoustic impedance contrasts in the area, which should result in anomalously high amplitude values at these interfaces. Based on this, amplitude iso-shells were created using cut-offs that highlighted a correlation between a high amplitude seismic reflector with the z lens mineralization within the prospective zone. Based on these iso-shells, a new potential target was identified further down plunge of the controlling structures.

Limitations in the effectiveness of the seismic brought about by the position of the prospective area sitting in the bottom corner of the seismic cube affect the quality of a definitive interpretation. However, the interpretation exercises carried out and their apparent correlation with known structures show that seismic appears to be imaging the key geology in the area and has the potential to be used as a viable exploration technique.

A number of recommendations are made to improve future interpretation work on data acquired from the Rosebery minesite:

- Careful design of future surveys allowing for the maximum chance to achieve the objectives of the survey
- Utilising the 3DPSTM AGC processing for structural interpretation while using the amplitude-consistent processing for amplitude anomaly identification
- Integrating results from subsequent drilling or geophysics

Contents

Executive Summary.....	1
Introduction	1
Software.....	1
GOCAD Mining Suite	1
Datasets	3
Coordinate System.....	3
Seismic Datasets	3
Seismic Amplitude Cube	3
Cosine Perigram	3
Instantaneous Phase.....	4
Geologic Datasets	4
Models	4
Boreholes	4
Interpretation	5
Conclusions and Recommendations for Future Interpretations	10

Figure 1: GOCAD 3D viewer with multiple datasets displayed.	2
Figure 2: Geologic models in 3D space. Primary structures identified.	4
Figure 3: Drillholes coloured by stratigraphy with lead-zinc assay spikes circled.	5
Figure 4: 3DPSTM AGC section with the Mount Black Fault in yellow, mineralisation surface in red and the Rosebery fault in blue.	6
Figure 5: 3DPSTM AGC instantaneous phase.	7
Figure 6: Fold map at approximate depth of interest (1100 m).	8
Figure 7: Iso-shells created from the AC processed cube. Z lens is circled in red and a potential down plunge target is circled in green.	9
Figure 8: 3DPSTM AGC section highlighting the geometric relationship of reflectors.	10

Introduction

This document contains 6 primary sections. An Executive Summary as seen above, this Introduction, a Software overview, a Dataset overview, Interpretation overview followed by Conclusions and Recommendations. Each section aims to define the processes involved in the interpretation phase of the Rosebery 3D seismic dataset.

The objectives of the interpretation were three fold:

4. Determine whether the seismic method was successful in imaging geology known to exist in the area.
5. Observe whether the mineralization was being directly detected by seismic in the form of amplitude anomalies.
6. Decide whether seismic was successfully imaging target geology further down dip.

Software

Interpretation of the Rosebery 3D seismic data set included the use of Paradigm's GOCAD Mining Suite for data display, dataset integration, the creation of 3D volume surfaces and structural interpretation. All outputs were saved in a Gocad project at the end of the interpretation session.

GOCAD Mining Suite

GOCAD Mining Suite was the primary interpretation software utilized. It offers the ability to integrate multiple geophysical and geologic datasets such as seismic cubes, electromagnetic data, satellite images, borehole information and previously interpreted surfaces and 3D volumes (*Figure 1*). This data is displayed in a user-defined coordinate system and provides the ability to slice through data in all orientations: in-line, cross-line, depth slices and arbitrary slices. Visually GOCAD allows variation and customization of amplitude colour spectrums and the ability to assign transparency to ranges of data, facilitating the display of multiple datasets at the same time.

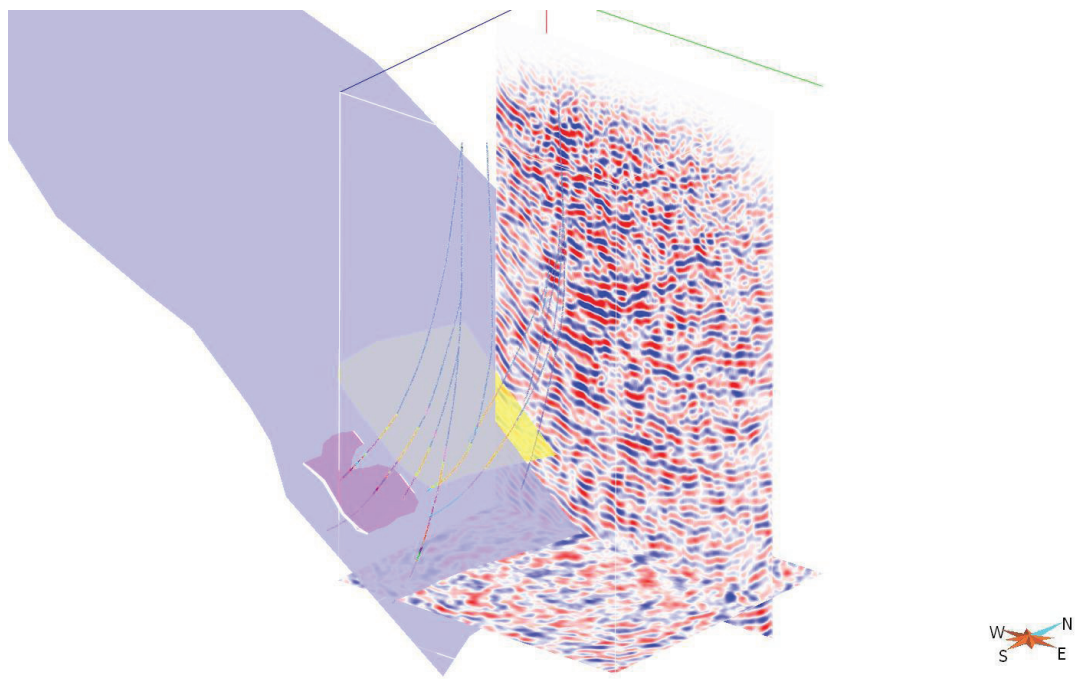


Figure 1: GOCAD 3D viewer with multiple datasets displayed.

Datasets

Coordinate System

The interpretation process involved the comparison and amalgamation of a number of datasets. These include geophysical, geological and borehole data. The interpretation was carried out in local mine coordinates but the seismic was acquired in GDA94. In order to perform the coordinate transformation in Gocad two reference points must be known in both coordinate systems. In the case of the Rosebery seismic data this is:

Name	GDA94			Local Mine Grid		
	Easting	Northing	elev	Easting	Northing	elev
ref 1	379391.3	5378631	0	1235.9	4102.336	3050
ref 2	379595.5	5377550	0	1224.3	3002	3050

An additional translation in the z-direction of +600 m was used to bring the seismic cubes to the seismic reference datum.

Seismic Datasets

A number of seismic datasets were provided to aid in the geologic interpretation of the data. These consisted of the primary *seismic amplitude cube* as well as a number of attributes generated from this.

Seismic Amplitude Cube

The seismic amplitude cube is generally used as the fundamental cube for carrying out a seismic interpretation. The seismic amplitude represents the contrast in acoustic impedance across geological interfaces and is therefore used to indicate lithology type at this position. Although many other factors influence the seismic response, the integration of more datasets and more information help to constrain the response and reduce the uncertainty.

In the case of the Rosebery dataset both a high resolution Automatic Gain Control (AGC) 3D Pre-Stack Time Migration (PSTM) cube was provided as well as a lower frequency amplitude-consistent (AC) 3DPSTM cube. The AGC cube utilises a harsh amplitude balancing tool that brings out subtle structures at the cost of reducing relative amplitude differences between seismic events. The AC cube works opposite to this in that it is processed to maintain relative amplitude differences between seismic events at the cost of resolution.

Initial processing also produced a Migration After Stack (MAS) cube that after comparison with the 3DPSTM cubes was deemed insufficient in terms of data quality for further use.

Cosine Perigram

Cosine perigram is the product of instantaneous amplitude and the coherency (similarity) coefficient multiplied by the cosine of phase. This attribute emphasizes the lateral continuity of strong events and is extremely useful in identifying structural features.

Instantaneous Phase

A derivative of the complex trace, instantaneous phase is used to enhance the lateral continuity of reflectors, especially in noisy areas. This attribute is particularly useful for aiding in horizon interpretation and observing the geometrical relationship between reflectors.

Geologic Datasets

Models

A number of geologic surfaces were provided by MMG geologists that represented previously interpreted structures from drillhole core logging. These included the key Rosebery (RF) and Mount Black Faults (MBF), which are believed to constrain the prospective zone of mineralization containing the Z lens mineralization. Other interesting features identified in core were also modeled and provided to observe whether they were correlatable with the seismic.

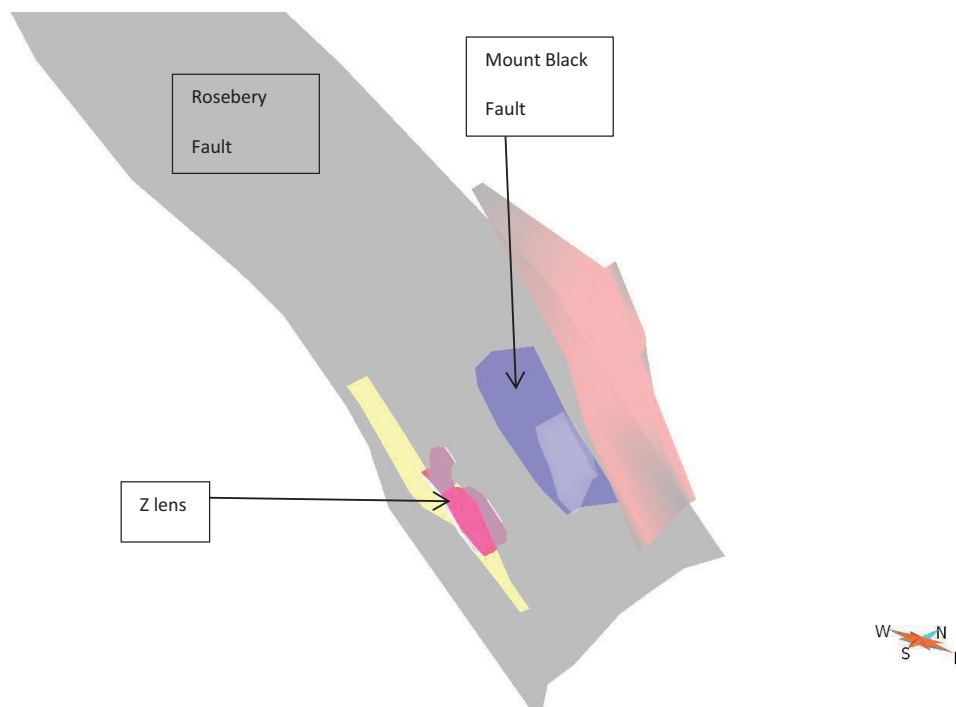


Figure 2: Geologic models in 3D space. Primary structures highlighted.

Boreholes

A drillhole database from the survey area was also provided by MMG (*Figure 3*). A number of these drillholes contained lithological zones interpreted from core, which are represented as coloured zones along the drillhole path. Assay data was also provided for these holes, which indicated the location of mineralization intercepts. This gave a reliable glimpse into the subsurface geology and was considered ground truth for the interpretation of the seismic data.

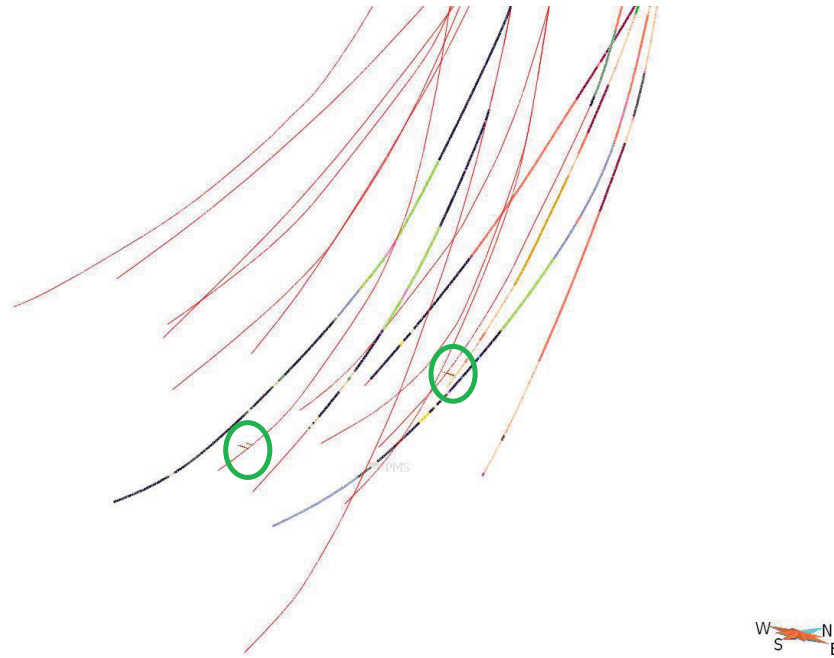


Figure 3: Drillholes coloured by stratigraphy with lead-zinc assay spikes circled.

Interpretation

A collaborative interpretation session was conducted over three days in the HiSeis office, Perth, Western Australia, beginning Wednesday 10th October, 2012. Geophysicists and geologists from both MMG and HiSeis spent 3 days interrogating the data with the objective of achieving a number of major outcomes. These were:

1. To determine whether the seismic method was successful in imaging geology known to exist in the area.
2. Observe whether the mineralization was being directly detected by seismic in the form of amplitude anomalies.
3. Decide whether seismic was successfully imaging target geology further down dip.

At the beginning of the session only the MAS cube was available for scrutiny. Unfortunately this was the lowest quality output and was found to be somewhat limited in what value it was able to add to the interpretation. Initial collaborative efforts were spent scrutinizing the MAS cube relative to subsurface information provided by MMG geologists in the form of drillholes and geological surfaces based on drill core interpretations.

Due to the inherent limitations in the post-stack migration algorithm, coupled with ambiguity in the z-direction of the cube due to a lack of velocity control to constrain the time-depth conversion it was difficult to carry out a credible analysis of whether the seismic method was successful in imaging the subsurface geology. It was at this stage that a 3D Pre-Stack Time Migration (PSTM) was decided to be run but due to the computer intensive nature of the algorithm preliminary results of a desampled cube were only made available towards the end of the interpretation session. Although promising,

there was no time to conduct an in-depth analysis of how well the cube managed to image the subsurface geology.

At the conclusion of the collaborative interpretation session HiSeis saw the need to attempt further processing streams beginning with re-running the 3DPSTM at 2 ms followed by running an amplitude-consistent processing flow.

The results of further processing made it clear that the 3DPSTM AGC cube would be best suited to carrying out a structural interpretation in the area in conjunction with the attributes generated from the AGC cube. This is due to the higher resolution provided by this particular processing stream and the improved imaging of subtle structures through the amplitude gain applied. For the case of Rosebery, the most useful attribute was found to be the instantaneous phase as it highlighted geometric relationships between the reflectors. These could be used to infer the presence of faults, such as the MBF and the RF.

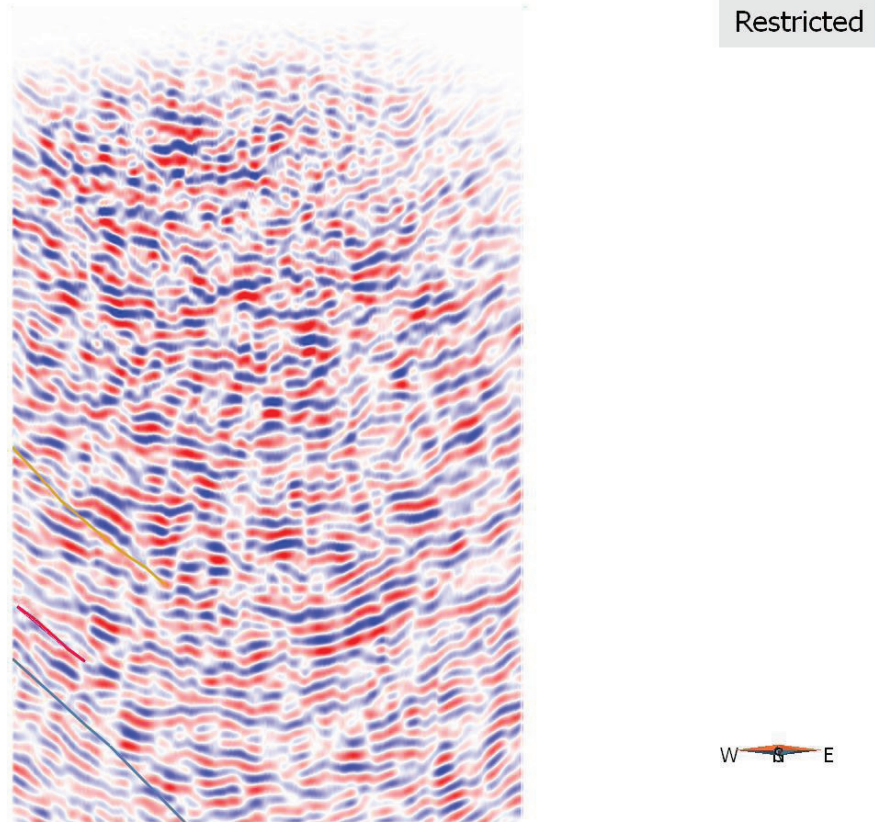


Figure 4: 3DPSTM AGC section with the Mount Black Fault in yellow, mineralisation surface in red and the Rosebery fault in blue.

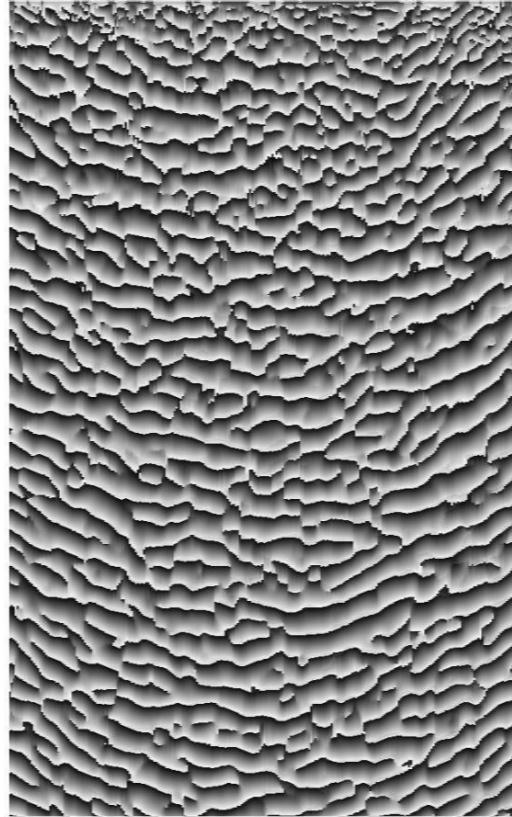


Figure 5: 3DPSTM AGC instantaneous phase.

Significant caveats are attached to the seismic data and should be made clear prior to an interpretation. Firstly, the prospective area occupies a region of the cube highly contaminated with processing artifacts. The bottom corner bounded by the RF and MBF is in a low fold portion of the cube (*Figure 6*) that contains migration artifacts known as ‘smiles’. When looking at a section, such as *Figure 4*, it can be seen that the edges of the section tend to pull up into what are commonly referred to as ‘smiles’. These are a consequence of the migration algorithm and not geologically related. However, in the case of Rosebery the target structures tend to dip in a similar orientation to these smiles. This makes interpretation of actual geological events more difficult and increases the reliance on geometrical relationships, such as those highlighted in the instantaneous phase cube, as well as auxiliary datasets such as the modelled surfaces based on drillhole intersections.

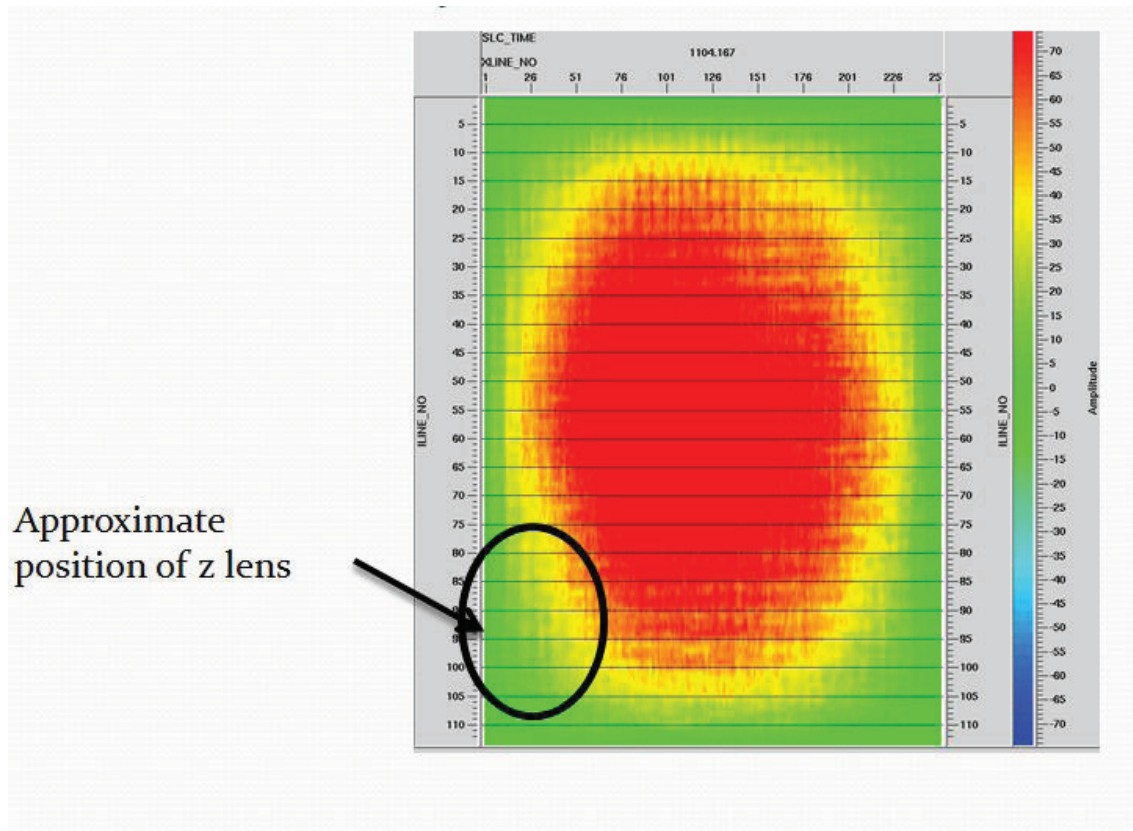


Figure 6: Fold map at approximate depth of interest (1100 m).

Based on physical rock property measurements it was established that the mineralisation was expected to provide a substantial acoustic impedance contrast with surrounding rock. This indicated the potential for mineralisation targeting via the identification of amplitude anomalies. To facilitate this an amplitude-consistent processing stream was carried out. The algorithms utilised in this stream aim to maintain relative amplitude differences between seismic events and therefore preserve strong amplitude responses brought about by variation in physical properties. From this strong amplitude responses observed in the AC cube could reliably be related to strong physical property contrasts, such as those expected to result from mineralisation. To aid in the identification of amplitude anomalies iso-shells were created in Gocad using an arbitrary amplitude value cut-off. This cut-off was based on what highlighted the known mineralisation best and then looking for similar amplitude signatures throughout the prospective area. Based on this technique, a new target was identified in the AC cube highlighted in *Figure 7*.

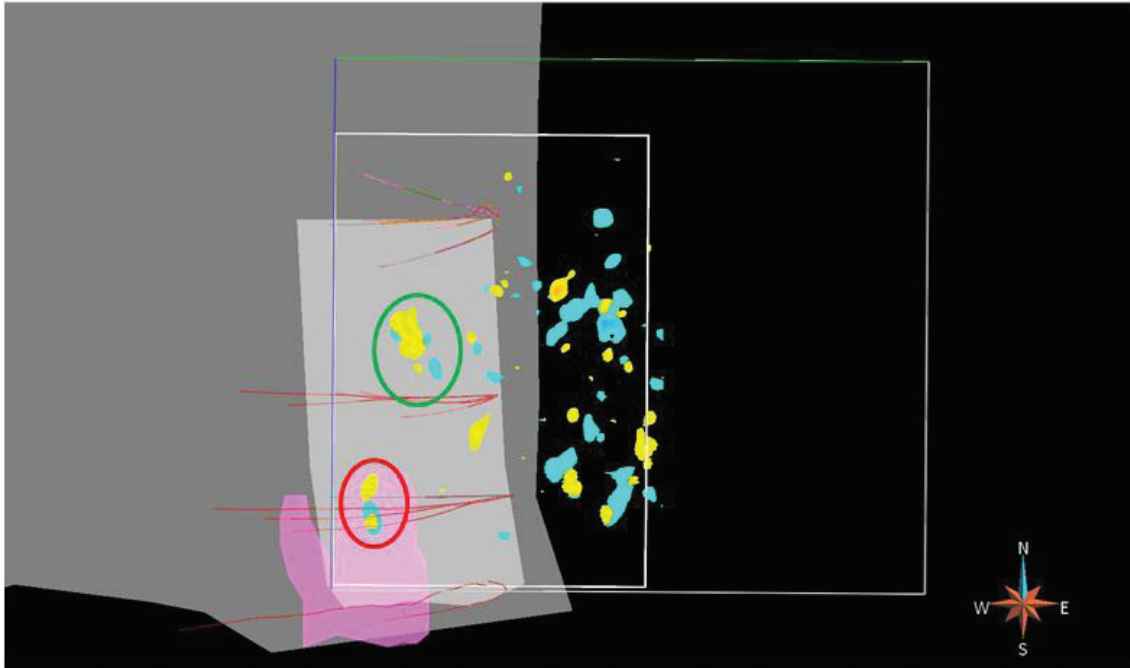


Figure 7: Iso-shells created from the AC processed cube. Z lens is circled in red and a potential down plunge target is circled in green.

HiSeis conducted an independent interpretation of the key surfaces (RF & MBF) using the 3DPSTM AGC and associated attribute cubes. The primary criteria for the identification of these faults were the geometric relationships of reflectors (*Figure 8*) and their intersections/truncations, which were particularly highlighted in the instantaneous phase attribute cube. This criteria was found to be particularly successful in picking out major fault structures, that correlated extremely well with modelled surfaces based on drillhole intersections.

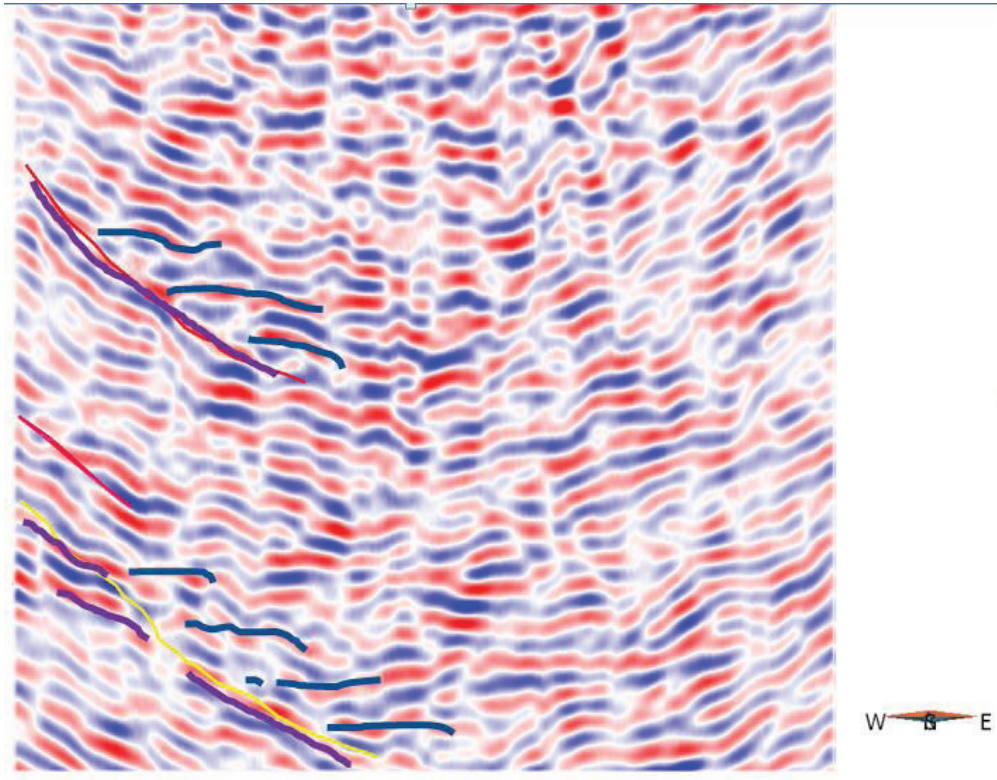


Figure 8: 3DPSTM AGC section highlighting the geometric relationship of reflectors.

Conclusions and Recommendations for Future Interpretations

An initial interpretation of the Rosebery 3D seismic data was conducted during an office visit by MMG personnel to the HiSeis office during the week beginning Wednesday 10th October, 2012. A subsequent interpretation conducted by HiSeis identified a number of fault surfaces, as well as a potential new down-plunge target. Due to the high complexity of the geology encountered and the limitations associated with the survey design identification of the key structures was difficult to carry out. However, reflector geometries provided an indication of potential structures that lined up well with surfaces modeled from drillhole intersections. Also, using the amplitude-consistent processed cube showed the correlation of a high amplitude event with the z lens mineralization. Based on this, a new potential target was also identified further down plunge. Therefore, it is believed that seismic is imaging the key geologic structures in the area and the potential for seismic as an exploration technique bears credence at the Rosebery minesite. A number of recommendations are made to improve further interpretations in the future:

- Careful design of future surveys allowing for the maximum chance to achieve the objectives of the survey
- Utilising the 3DPSTM AGC processing for structural interpretation while using the amplitude-consistent processing for amplitude anomaly identification
- Integrating results from subsequent drilling or geophysics

APPENDIX D: HISEIS INTERPRETATION REPORT

HiSeis Pty Ltd.
Suite 4, Enterprise Unit 3
9 De Laeter Way
Bentley WA 6102
Australia



Processing Report

Rosebery High Resolution 3D Seismic Survey *Rosebery, Tasmania*

For

Minerals and Metals Group Limited.

Report number: MMG-3DROSEPROC12

Prepared by

Jai Kinkela

April 2013

Executive Summary

An experimental 3D seismic survey was acquired at Rosebery, Tasmania, from February – August 2012 on behalf of Minerals and Metals Group Limited in order to identify the major structures associated with lead-zinc mineralisation and if possible directly target mineralisation itself.

Data was acquired in GDA94 using explosives as the seismic source over an area of approximately 2 km². The explosives were found to provide ample signal when coupled with fresh rock but was borderline when coupled with saturated, marshy ground. An extreme elevation profile resulting from acquiring data on the side of a mountain along with a poor signal-to-noise ratio due to significant swaths of data affected by raindrop noise made for challenging acquisition and processing conditions from the beginning. A final reference datum of +600 m ASL was used. The survey design and parameters made imaging the target structures difficult due to the spatial position of the target and limited offsets of the small acquisition area.

The 3D grid was processed utilising a processing flow adapted to the acquisition parameters, survey objectives and geology known to exist at the Rosebery survey area. Significant processing efforts were needed to combat areas of low signal to noise ratio, a large amount of unacceptably noisy traces, extreme topography as well as a deep and dipping target that made migration difficult.

A number of migration algorithms, including post and pre-stack, were attempted in order to image the steeply dipping and deep target structures on the edge of the survey area. A 3DPSTM (pre-stack time migration) was found to best image these structures and was used for further processing.

A processing flow utilising an automatic gain control (AGC) was used to balance amplitudes and enhance subtle features. An alternate amplitude-consistent processing flow was also run in order to maintain relative amplitude values to allow for the direct targeting of mineralisation through the identification of amplitude anomalies.

Attributes were generated from the cube created using the AGC processing flow in order to aid the interpretation of the data. These were namely instantaneous phase and perigram multiplied by the cosine of phase.

Taking into consideration the challenges and limitations effecting the data the final processing results showed that seismic methods can be used for mapping important structures in this exploration area.

Recommendations for the data and future surveying in the area include:

- Further exploration may benefit from a larger survey to achieve improved imaging and a better understanding of the complex underground structures through the incorporation of a wider range of offsets
- The acquisition of Vertical Seismic Profiling (VSP) and Full Waveform Sonic (FWS) to better constrain the time-depth conversion velocity field as well as determine whether the mineralisation is reflecting to surface

Contents

Executive Summary.....	i
Introduction	1
Acquisition	1
Overview	1
3D Processing.....	5
Overview	5
Pre-Processing.....	5
AGC Data Processing.....	6
Velocity Analysis	9
Migration	10
Amplitude-consistent processing	11
Seismic Attributes	12
Instantaneous Phase.....	12
Perigram * cosine of phase.....	13
Conclusions and Recommendations.....	14
APPENDIX A – Seismic Data Processing – An Overview.....	15
.....	24

Figure 1 - Original 3D Survey Design (Receivers Green, Sources Red)	3
Figure 2: Final surveyed receivers and shot points coloured based on elevation.....	4
Figure 3: Fold map for binning at 10 m x 5 m.	7
Figure 4: Raw shot record with noisy traces killed (above) compared to shot record with refraction statics + pre-processing (steps 2 – 12) (below) applied.....	8
Figure 5: An example of the RMS velocity field from a representative inline that was used for stacking. Velocities generally range from 3700 m/s – 5200 m/s.....	9
Figure 6: Post-stack migrated cube in local mine coordinates. Area of interest circled in green.	10
Figure 7: Pre-stack time migrated cube in local mine coordinates. Area of interest circled in green.	11
Figure 8: Amplitude-consistent cube in local mine coordinates. Area of interest circled in green.	12
Figure 9: Instantaneous phase attribute cube in local mine coordinates.	13
Figure 10: Perigram multiplied by the cosine of the phase attribute cube in local mine coordinates.	14

Introduction

This final processing report is divided into six main sections: the Executive Summary (above), this Introduction, Acquisition, 3D Processing, Additional Processing and Conclusions and Recommendations. Each section outlines specific data, summaries and explanations relating to all aspects of the seismic processing carried out for the 3D dataset acquired at the Rosebery survey area.

Acquisition

Overview

The acquisition phase includes all of the in-field equipment and survey preparation as well as the physical acquisition of the seismic data itself. This is comprehensively covered in the **Acquisition Report (MMG-3DROSEACQ12)**. The acquisition phase took place between the months of February and August 2012. The original and actual survey design is illustrated in *Figure 1 & Figure 2*. Explosives were used as the seismic source for the survey with all receiver and source points measured in coordinate system **GDA94**.

Parameter	Final
Total Acquisition Area	~2 km ²
Number of Receiver Lines	20
Live Channels/Patch (Nominal)	960
Live Receiver Lines/Patch	10
Live Channels/Receiver Line	96
Receiver Interval (In-line)	10 m
Receiver Interval (X-line)	100 m
Nominal Receiver Density	1111.1 per km ²
Total Source Points	1975
Total Unique Source Locations	1776
Nominal Shot Point Density	397.2 per km ²
Number of Source Lines	20
Source Interval (In-line)	10 m & 20 m
Source Interval (X-line)	80 m
Record Length	3 s
Sample Rate	2 ms
Source Type	Explosives

Table 1 - Final survey parameters



Figure 1 - Original 3D Survey Design (Receivers Green, Sources Red)

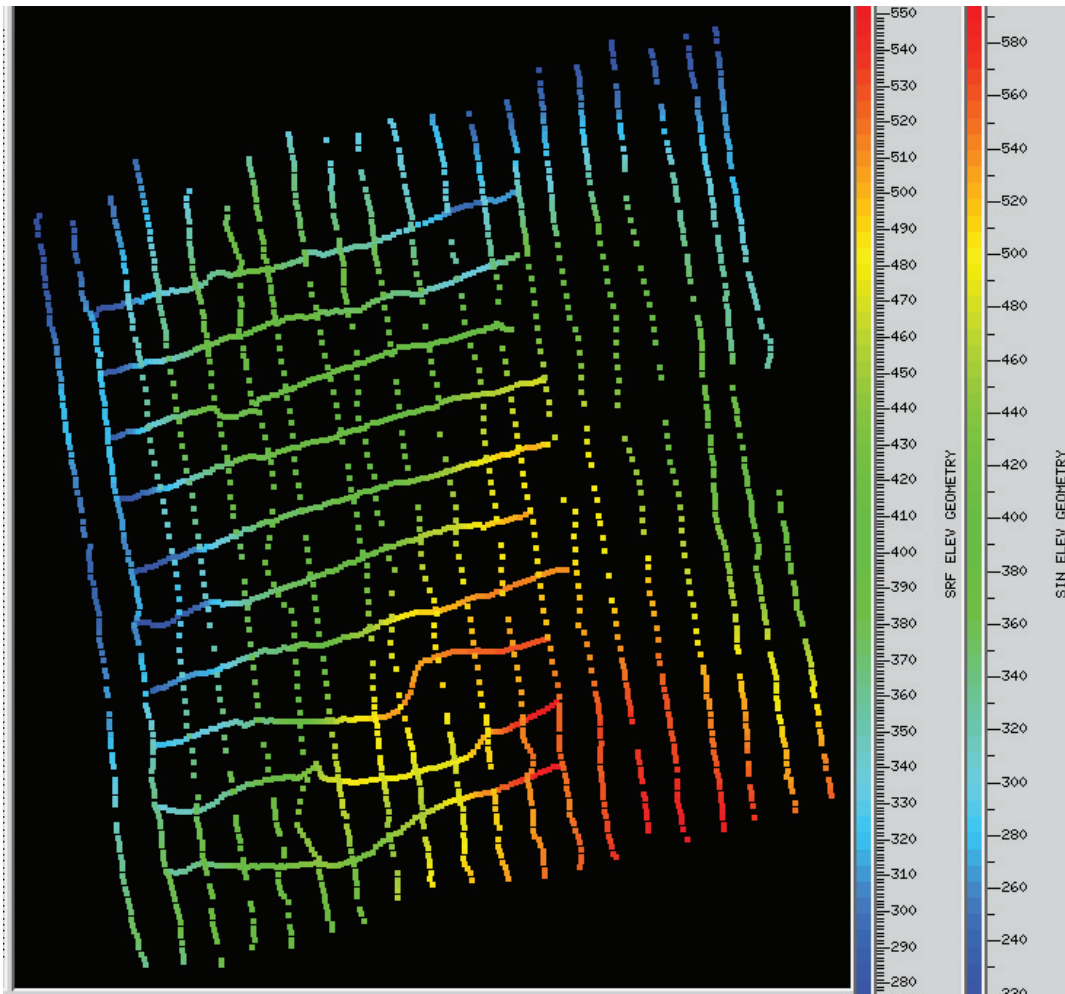


Figure 2: Final surveyed receivers and shot points coloured based on elevation.

3D Processing

Overview

Processing of the Rosebery 3D dataset involved a number of key steps that are discussed in more detail in the following sections. In the case of Rosebery where the target structures are steeply dipping, at depth, and towards the edge of the survey area, the main processing effort was put into the testing of various migration algorithms. Along with this, two significantly different processing streams were carried out to emphasize certain characteristics of the seismic data. The first stream aimed to enhance subtle amplitude events through the utilization of an Automatic Gain Control (AGC). This was designed to aid structural interpretation by enhancing subtle structures within the cube. The other aimed to maintain relative amplitude differences in order to emphasize amplitude anomalies, such as those expected to result from mineralisation.

Pre-Processing

Pre-processing involves those steps that are required to 'clean' the data, removing bad traces and prepare the data for actual processing. Often this phase proves to be one of the most time-consuming aspects of the processing sequence. This tended to be the case for the Rosebery 3D dataset.

Firstly, observers logs that provided a hard copy of every shot record, geometry and issues faced in the field were digitised for ease of access. This performs two functions: namely QCing of each shot record through cross-referencing with the digitised observers log to remove bad, questionable or repeated shots and facilitating the preparation of data for the seismic processing to begin.

Geometry was assigned to each channel, where coordinate information and the source point - receiver point relation are established and entered into the headers. As the survey consisted of a single 3D patch geometry was a relatively easy procedure to establish.

Trace editing was carried out to remove bad or noisy traces that may reduce the overall signal-to-noise ratio of the seismic data. By far the biggest source of noise on the spread was raindrop noise, both from the rain itself as well as rain collecting in the rainforest canopy. This caused prolonged noise even after the rain had passed. The application of particular noise-spike removal algorithms to the shot records helped to identify and remove traces affected by raindrop noise.

First break picking was then carried out to facilitate the calculation of refraction statics. This is an often tedious and time consuming process whereby every shot record (approximately 1750 in the case of Rosebery) has its first arrival picked allowing the time delays due to the weathered zone to be calculated. This is designed to remove the harmful velocity variations of the heterogeneous regolith. In the case of Rosebery, it is believed the regolith doesn't extend too far beneath the surface. Instead, the fact that the survey area was on the side of a mountain meant that accounting for elevation statics would be a more crucial step. It was found that elevations varied from approximately 262 m – 556 m ASL.

Due to this, **the seismic data was referenced to a datum of +600 m ASL.**

AGC Data Processing

The full processing flow for the AGC processing stream is outlined in *Table 2*.

1. Binning (10 m x 5 m)
2. Trace editing and noise-spike removal
3. Refraction static computation (Delay time and diminishing residual matrix) and second edit of first break picks
4. Quality control (QC) of the refraction static solution (on shot records, every 20 th shot)
5. Application of refraction statics
6. Window design for amplitude compensation and deconvolution
7. Tests for: amplitude compensation, band-pass filter, Multi-channel filtering (F-K/ τ -p), autocorrelation and deconvolution
8. Application of ensemble balance and spherical divergence correction
9. Application of spiking deconvolution – zero phase spiking, 80 ms operator, 0.1% white noise
10. Surface wave noise attenuation: 2200 m/s
11. Airblast attenuation: 330 m/s
12. Application of band-pass filter: 8 – 14 – 125 – 200 Hz Ormsby
13. constant velocity stacks (CVS)
14. NMO application
15. Brute stack
16. Computation of surface consistent residual reflection statics (QC check)
17. Application of residual statics
18. Residual stack I
19. Second pass velocity analysis (CVS)
20. Residual stack II
21. PSTM: 80% stacking velocities, maximum dip 50 degrees, absolute offset of first bin centre 20 m, bin size 40 m, maximum offset 1786
22. Inverse TAR applied
23. Stack
24. Seismic attribute cubes calculated
25. time/depth conversion
26. SGY files to specification

Table 2: AGC Processing Flow

Refer to **Appendix A** for an overview of the theory behind the seismic processing steps taken.

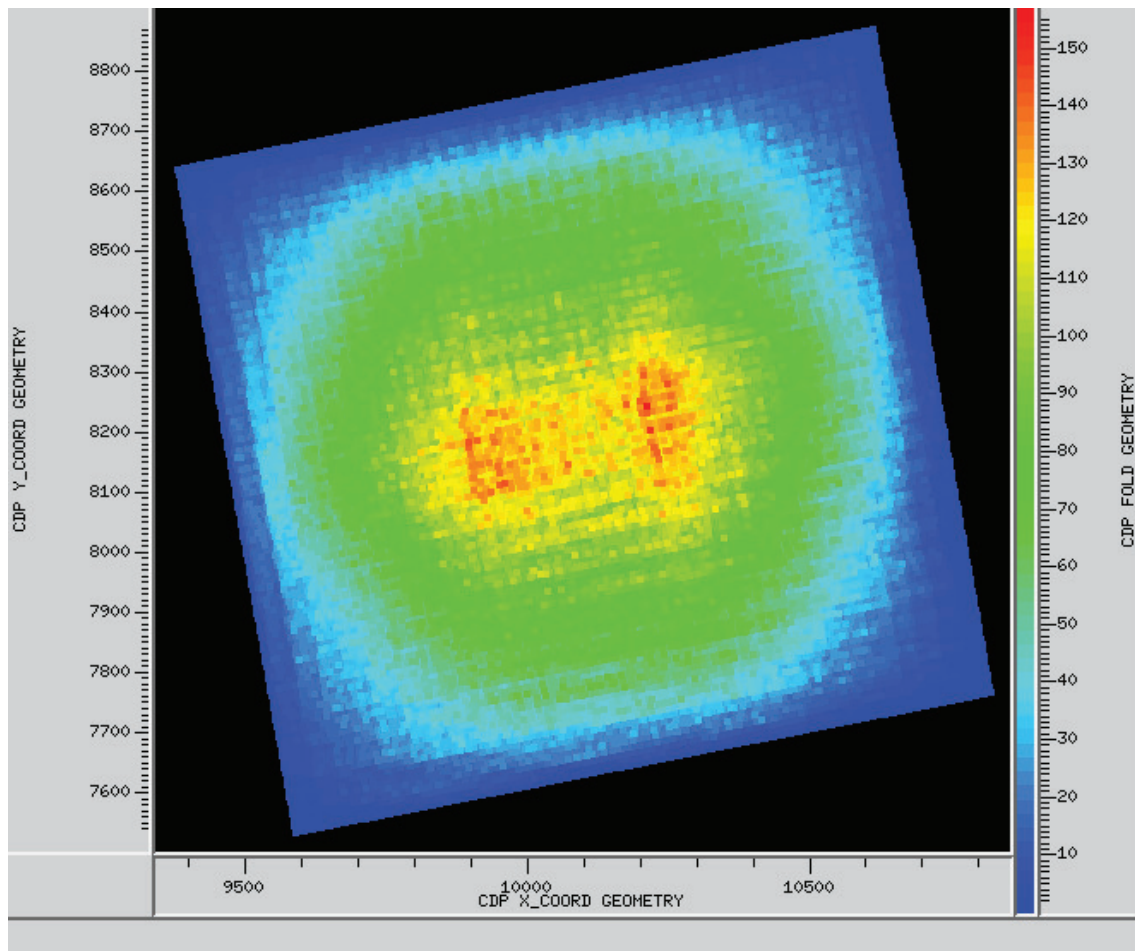


Figure 3: Fold map for binning at 10 m x 5 m.

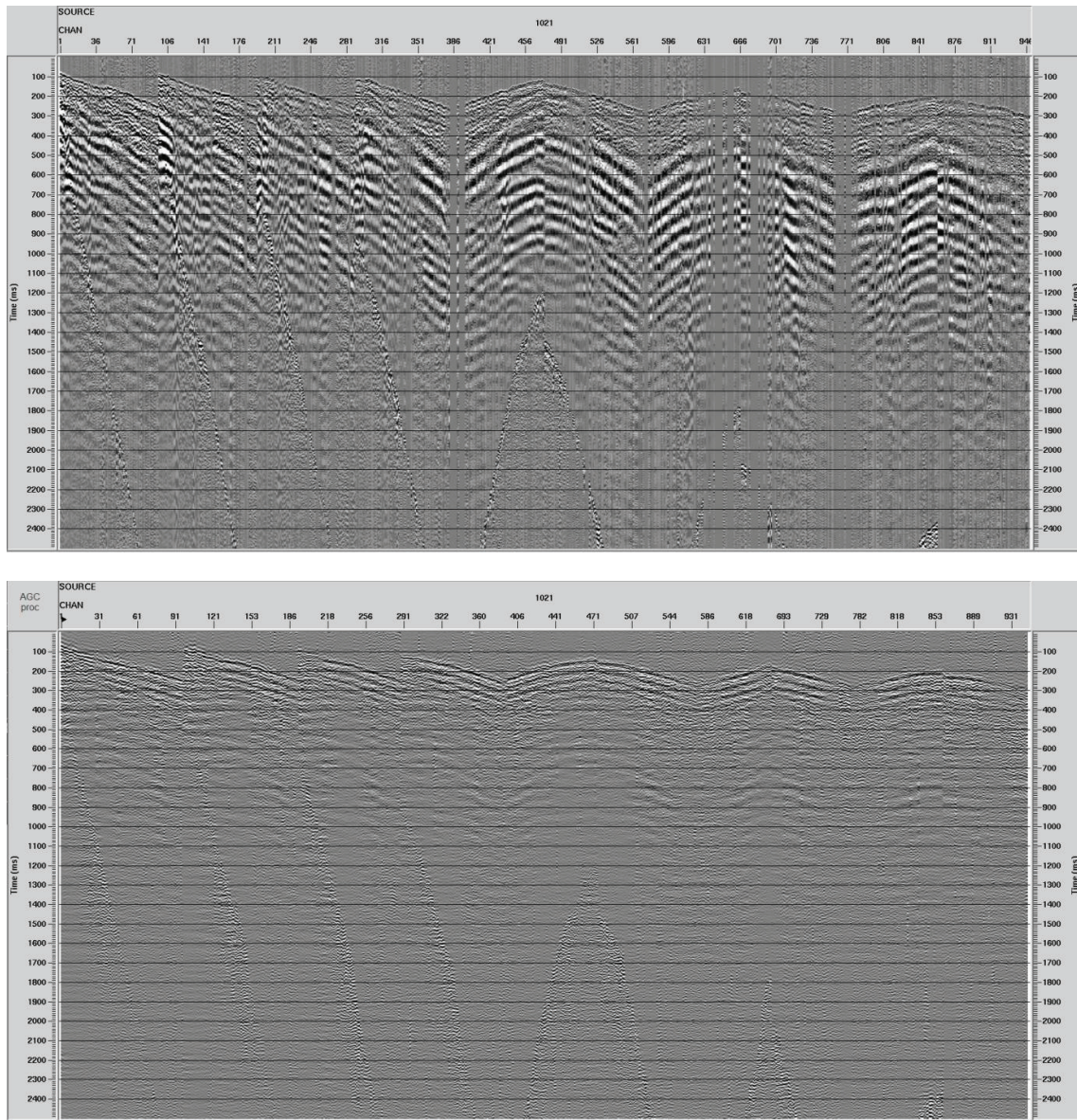


Figure 4: Raw shot record with noisy traces killed (above) compared to shot record with refraction statics + pre-processing (steps 2 – 12) (below) applied.

Velocity Analysis

A critical step in hard-rock seismic processing is velocity analysis. Due to a number of reasons, interactive (semblance) velocity analysis (IVA), which is commonly used in oil & gas soft rock environments, is deemed insufficient as a stand alone velocity analysis tool. Often a lack of signal-to-noise ratio and a lack of laterally continuous and coherent events in hard rock seismic data reduces the effectiveness of the IVA technique. Therefore, velocity analysis was initially carried out using the Constant Velocity Stacks (CVS) technique with further refinement provided by IVA. With regards to the CVS technique, a preliminary understanding of expected rock velocities in the area must be known so as to better differentiate between real and artificial events.

CVS involves stacking common depth points (CDPs) using a varying single velocity, which when compared to one another will show some events more prominently than others. This indicates that a particular velocity has better stacked the event at this position and hence the velocity-time pair for this particular CDP can be established.

Once a velocity function has been determined for a number of CDPs, these can be used to create the stacking velocity field from which the brute stack will be created (*Figure 5*).

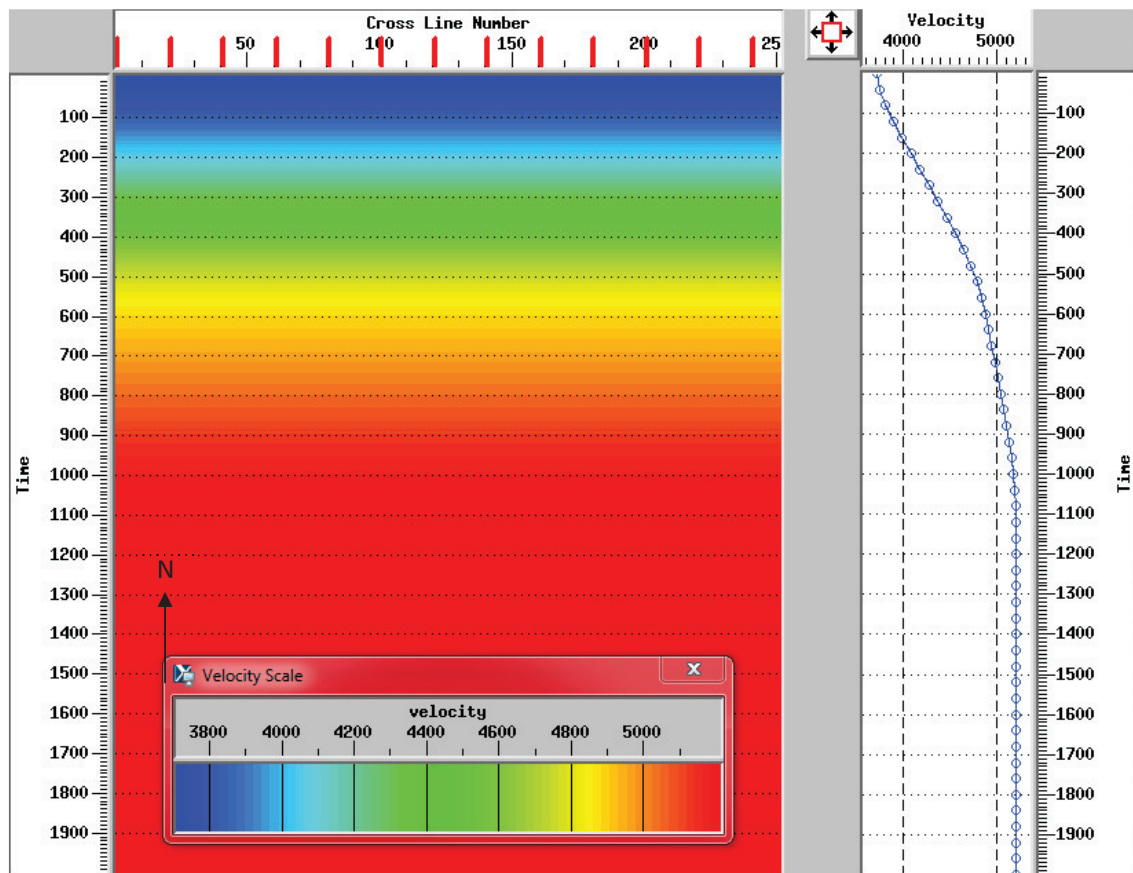


Figure 5: An example of the RMS velocity field from a representative inline that was used for stacking. Velocities generally range from 3700 m/s – 5200 m/s.

Migration

A number of migration algorithms were attempted in order to determine which worked best for the data. Limitations brought about by complexities in the survey design were found to impact the effectiveness of certain algorithms. The limitations faced were namely the steep dip of the target structures, their position relative to the survey area and the offsets available within the survey area. The combination of these factors made it very difficult to image the target geology.

Firstly, a post-stack migration was applied but was found to be unsatisfactory. Due to this particular algorithm being less rigorous in nature, results are achieved much faster but quality suffers in the presence of lower quality data. In the case of Rosebery and hard rock environments in general an intrinsically low signal to noise ratio reduces the effectiveness of any velocity analysis carried out. As migration is sensitive to the velocities used this negatively impacts the quality of the migrated section. This, in tandem with the spatial position of the target structures being on the edge of the survey area and such a large variation in topography make it difficult to accurately migrate them to their true position.

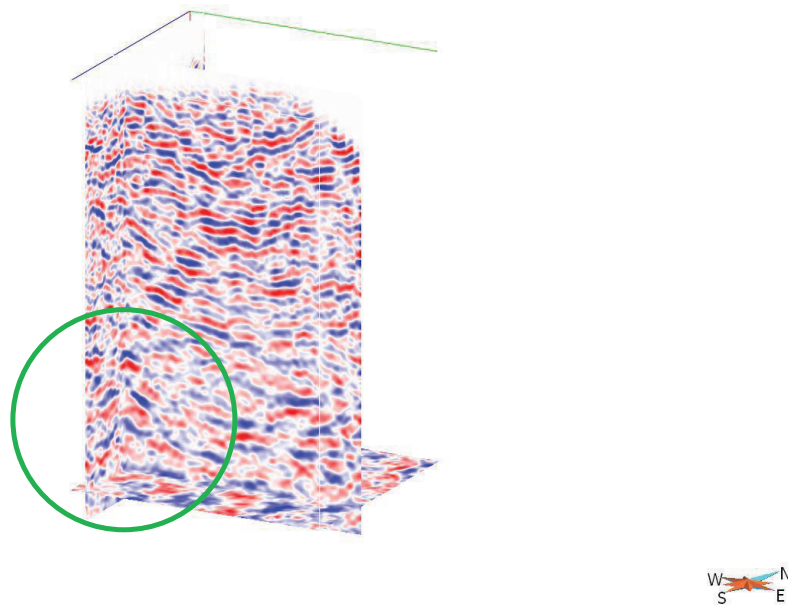


Figure 6: Post-stack migrated cube in local mine coordinates. Area of interest circled in green.

In light of the results of the post-stack migration a Pre-Stack Time Migration (PSTM) was attempted as well. Known to be a more rigorous migration algorithm, the results of this processing was found to be far superior compared to the post-stack migrated cube, particularly at depth and in the area of interest. An 80% scaling factor of migration velocities was necessary to be used so as to give the target geology the best chance of being imaged within the limited extents of the survey area. A consequence of these velocities is that they may lead to inaccuracies in reconstructing the true dip of geologic events.

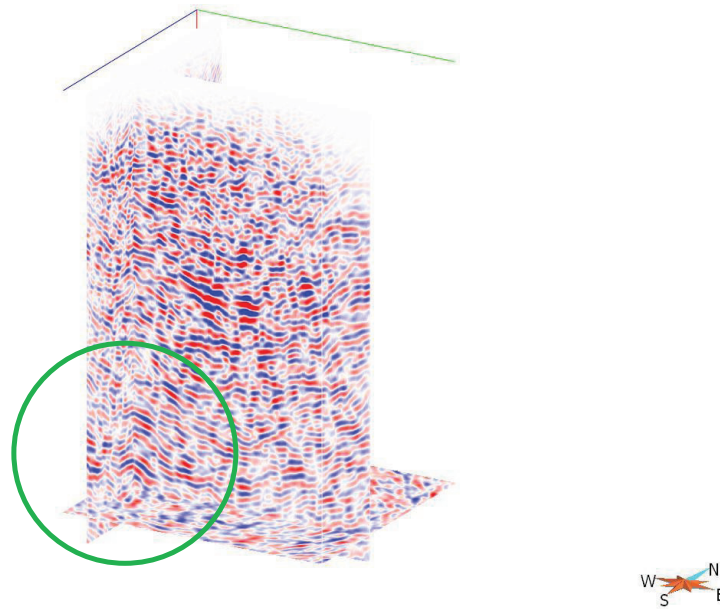


Figure 7: Pre-stack time migrated cube in local mine coordinates. Area of interest circled in green.

A time – depth conversion velocity field was created from the migration velocity field as a smooth average function (table 3) until more velocity information such as one obtained from Vertical Seismic Profiling (VSP) becomes available. Based on structural surfaces provided by MMG a scaling factor of 110% was arbitrarily applied. It is important to note that the time – depth velocity field is still open to modification.

Amplitude-consistent processing

An amplitude-consistent (AC) processing stream was also applied to the data in order to maintain relative amplitude variations for the purpose of direct targeting of massive sulphides. Based on physical rock property measurements, the target mineralisation is expected to provide a large acoustic impedance contrast, manifesting in anomalously large amplitudes in comparison to surrounding rock. The processing flow is outlined in *Table 3*:

Amplitude-consistent processing flow

- | | |
|-----|---|
| 1. | Binning (10 m x 5 m) |
| 2. | Trace editing and noise-spike removal |
| 3. | Refraction static computation (Delay time and diminishing residual matrix) and second edit of first break picks |
| 4. | Quality control (QC) of the refraction static solution (on shot records, every 20th shot) |
| 5. | Application of refraction statics |
| 6. | Ensemble balance |
| 7. | Surface consistent amplitude recovery - computation |
| 8. | Surface consistent amplitude recovery - application |
| 9. | Surface wave noise attenuation: 2200 m/s |
| 10. | Surface consistent deconvolution – spiking 80 ms gap, 0.1% white noise operator |
| 11. | Airblast attenuation: 330 m/s |
| 12. | Application of band-pass filter: 10 – 15 – 120 – 160 Hz Ormsby |
-

13.	TFD noise rejection – window 20 ms, aperture 5, threshold multiplier 3
14.	NMO application
15.	Brute stack
16.	Computation of surface consistent residual reflection statics (QC check)
17.	Application of residual statics
18.	Residual stack I
19.	Second pass velocity analysis (CVS)
20.	Residual stack II
21.	PSTM: 80% stacking velocities, maximum dip 50 degrees, absolute offset of first bin centre 20 m, bin size 40 m, maximum offset 1786
22.	Inverse TAR applied
23.	Stack
24.	Seismic attribute cubes calculated
25.	time/depth conversion
26.	SGY files to specification

Table 3: AC Processing Flow

The results of the AC processing resulted in a cube of reduced resolution but with the inclusion of some new amplitude anomalies (*Figure 8*).

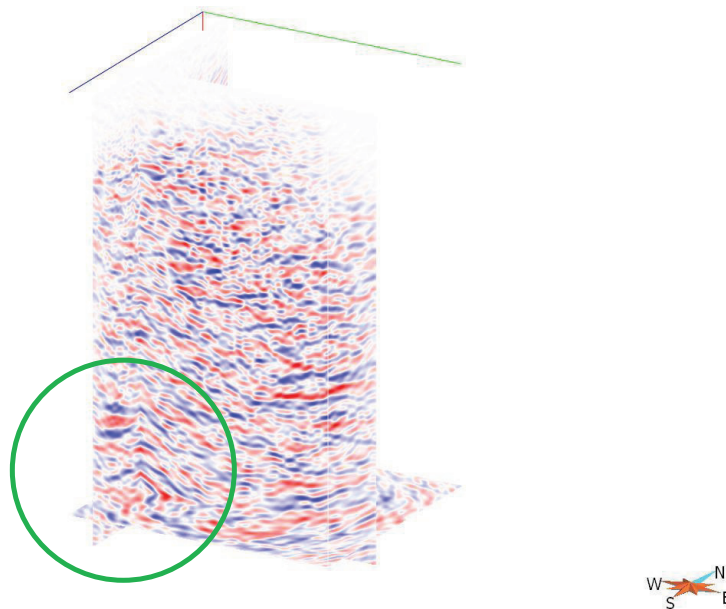


Figure 8: Amplitude-consistent cube in local mine coordinates. Area of interest circled in green.

Seismic Attributes

In order to aid in the interpretation of the seismic sections a number of seismic attributes were generated. These include:

Instantaneous Phase

A derivative of the complex trace, instantaneous phase is used to enhance the lateral continuity of reflectors, especially in noisy areas. This attribute is particularly useful for aiding in horizon interpretation and observing the geometrical relationship between reflectors.

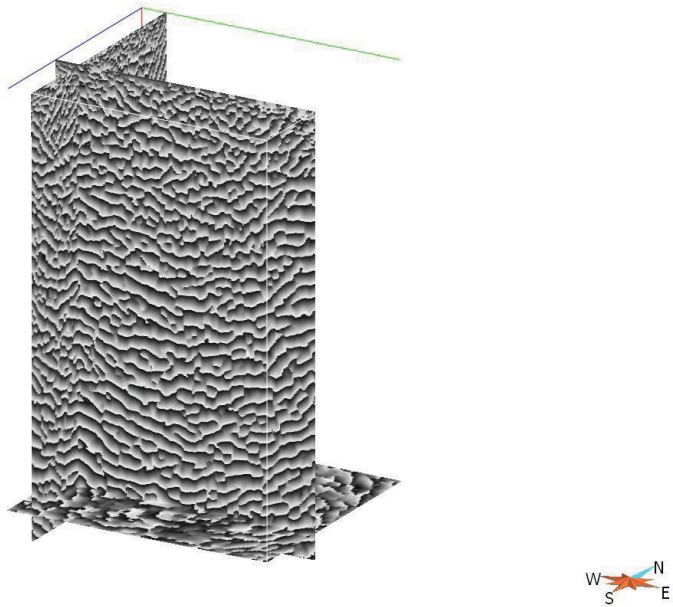


Figure 9: Instantaneous phase attribute cube in local mine coordinates.

Perigram * cosine of phase

A low-pass filter is applied to the reflection strength multiplied by the reflection continuity and is used to emphasize the lateral continuity of strong events. This is extremely useful in identifying structural features.

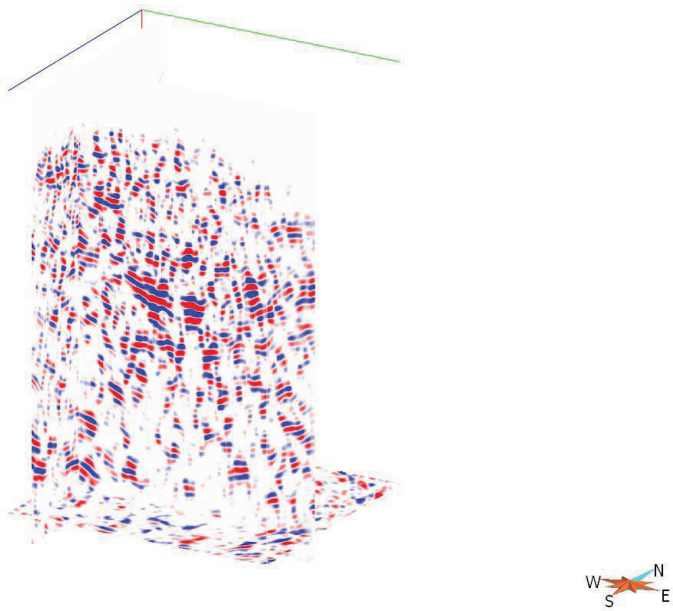


Figure 10: Perigram multiplied by the cosine of the phase attribute cube in local mine coordinates.

Conclusions and Recommendations

A relatively small sized 3D survey was acquired at Rosebery, Tasmania, that demonstrated the high potential for the application of seismic reflection methods for mineral exploration at this site.

Despite a poor signal-to-noise ratio, deep and steeply dipping target structures situated at the edge of the survey area and extreme topography the processing was able to image a number of seismic events of interest. This was achieved through the testing of multiple migration algorithms as well as processing streams to determine what was most suitable for the challenges known to exist in the area.

The 3DPSTM AGC cube was found to provide the best resolution and continuity of seismic events, and is therefore recommended for carrying out a structural interpretation. Multiple attributes were generated from this cube, such as instantaneous phase and preigram multiplied by the cosine of phase, to aid in the interpretation of the seismic data.

The 3DPSTM amplitude-consistent cube was processed to maintain relative amplitude variation between lithologies and would therefore be useful in highlighting amplitude anomalies such as those expected to result from mineralisation.

Recommendations for the data and future surveying in the area include:

- Further exploration may benefit from a larger survey to achieve improved imaging and a better understanding of the complex underground structures through the incorporation of a wider range of offsets
- The acquisition of Vertical Seismic Profiling (VSP) and Full Waveform Sonic (FWS) to better constrain the time-depth conversion velocity field as well as determine whether the mineralisation is reflecting to surface

APPENDIX A – Seismic Data Processing – An Overview

The processing of seismic reflection data involves numerous mathematical operations. These, however, can be grouped into three main categories:

- I. Time corrections*
- II. Signal to noise improvement*
- III. Repositioning or inverse modelling*

Time corrections:

- a) **Static corrections** These aim to equalise travel times through the typically low velocity near surface weathered layer or so-called regolith in hard-rock environment. For this computation we utilise waves which totally refract at the weathering/fresh rock interface. This wave is a “diving” wave (**Figure A1**). For land seismic data this step is of crucial importance since time delays through the regolith layer could completely misalign reflected signals and result in destructive summation during the process of stacking. Computed refraction statics cannot however fully compensate the travel time differences through the weathered layer (regolith) due to the nature of head waves which are “diving” through highly rugose intervals (**Figure A1**). Consequently additional computations are required to fine-tune reflection events.
- b) **Residual statics:** These are conventionally computed using reflection events, again in a surface consistent manner. We can also use here a modified procedure, which we developed recently for the case of a low fold data and very weak signal. The procedure consists of the following steps:
 - Time-correct refracted events using linear equations (linear moveout or LMO) with a velocity of the fresh rock derived under step a).
 - Sort and stack refraction events.
 - Pick horizon along refractions and select time window that encompasses only refracted events.
 - Compute residual statics using the algorithm devised for reflection data.

c) Dynamic corrections involve flattening reflection hyperbolae with appropriate velocity (NMO velocity for short offset) in preparation for data summation (**Figure A2 and A3**). The correction is based on the travel time equation (**Figure A2**) which is derived for a single layer, constant velocity case. The same equation is valid for a multi layer case as long as they are horizontal. The actual correction is implemented on a sample by sample basis using the normal-move-out (NMO) equation (**Figure A3**). Before this step can be carried out we need to define the velocity of the layers. Clearly the “best” velocity will be the one which flattens reflection hyperbolae. This “flattening” or search for the best velocity involves interactive velocity analysis (**Figure A4**). Velocities are typically analysed in regular intervals along seismic line.

Signal to noise improvement:

This sequence of processes involves a large number of diverse mathematical operations. They are however all aimed to improve the signal-to-noise ratio. Initial steps here are compensation of reflection amplitudes. Two main types of amplitude corrections aim to compensate losses due to natural wavefront spreading and losses at each interface (reflection, refraction and mode conversion processes). While the first correction is readily specified, the latter one is of an exponential type but hard to determine explicitly (**Figures A5 and A6**). Consequently the total amplitude correction is estimated by testing and visual inspection.

A large group of operations is aimed at removing all but primary reflection energy from seismic data. These techniques are either single-channel operations such as band-pass filtering and deconvolution or multi-channel operations such as F-K filtering, tau-pi filtering, etc. The basic principles of these techniques with data examples are shown in **Figures A7 - A12**.

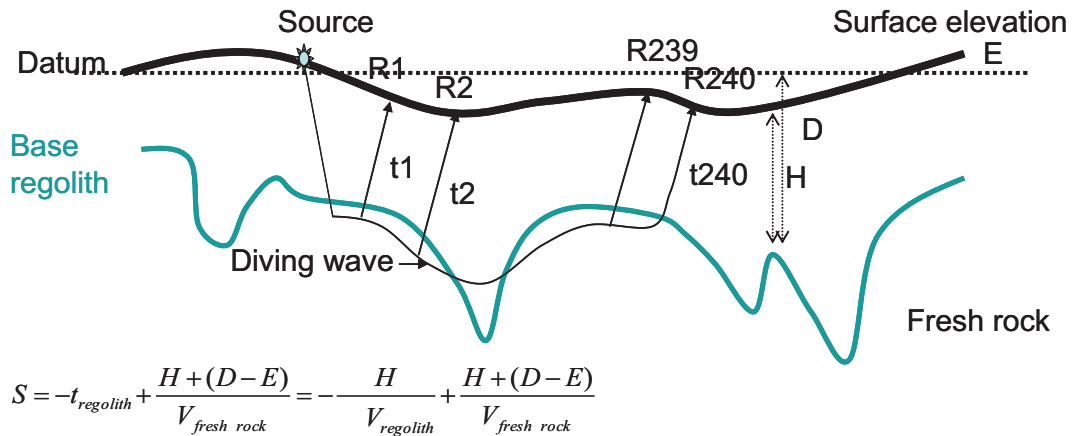
Finally the most powerful and the simplest technique we have for enhancing the primary signal is stacking. That is the summation of a number of traces which contain signal and originate from the same depth point for various source-receiver separations into one trace. Hence, in general the larger the fold the better the signal-to-noise ratio will be. The main problem with the stacking method is that it assumes that all of the traces, which go into summation, carry exactly the same information that is contained in the signal recorded from the same depth point. Strictly speaking this is only true for a layer-cake earth model. The summation process is effective even

for the dipping structures but it becomes discriminative if a range of different dips, particularly conflicting dips, are present in the data.

Repositioning or inverse modelling

If dipping events are recorded in the data they need to be repositioned in their true location since seismic traces are plotted vertically. This provides a geometrical explanation of the migration process (**Figure A13a**). The actual process after stack is accomplished by using the wave equation (inverse modelling) and commonly the exploding reflector principle for the imaging condition. All of the migration schemes naturally produce a depth section (true inverse modelling). In practice they are modified to produce time migrated images which contain no immediately recognisable errors, until the interpretation results (maps, horizons or time-section) are converted to depth.

STATIC corrections – travel time equalisation through weathered layer



t1-t2 = receiver static difference, reciprocity for shots
 Average (in various ways) 120/240 differences for each shot and receiver
 Various methods: ABS, Delay Time, GRM, DRM

Figure A1. Computation of travel times and weathering depth from totally refracted (head) waves. This is accomplished in a surface consistent manner, using reciprocity principle.

Dynamic corrections (NMO)

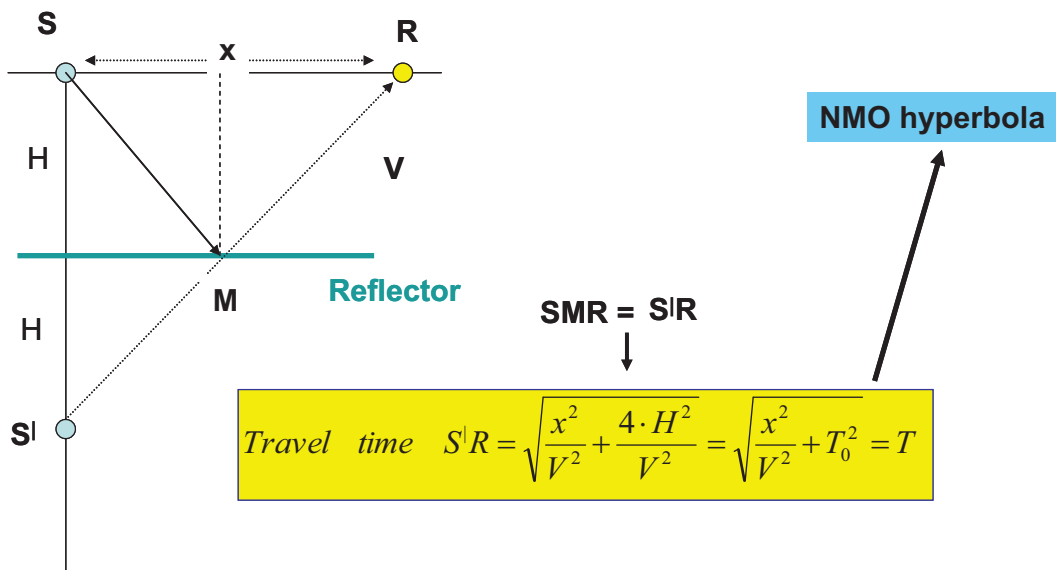


Figure A2. Travel time equation – reflection hyperbolae, derived for a single layer case. Note that S'R is square time as well as T.

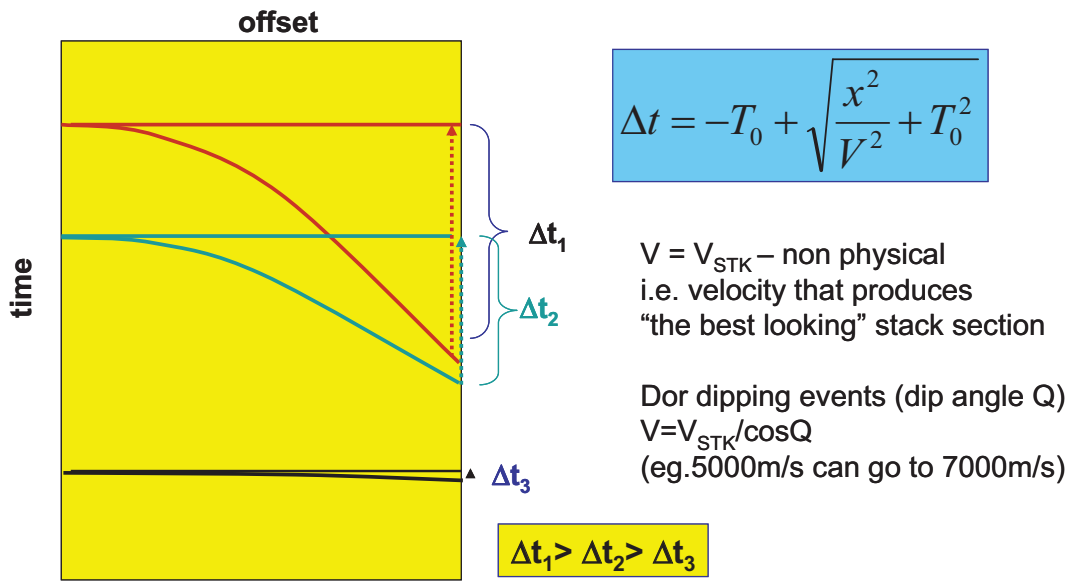


Figure A3. The actual dynamic correction Δt is known as normal moveout (NMO) correction.

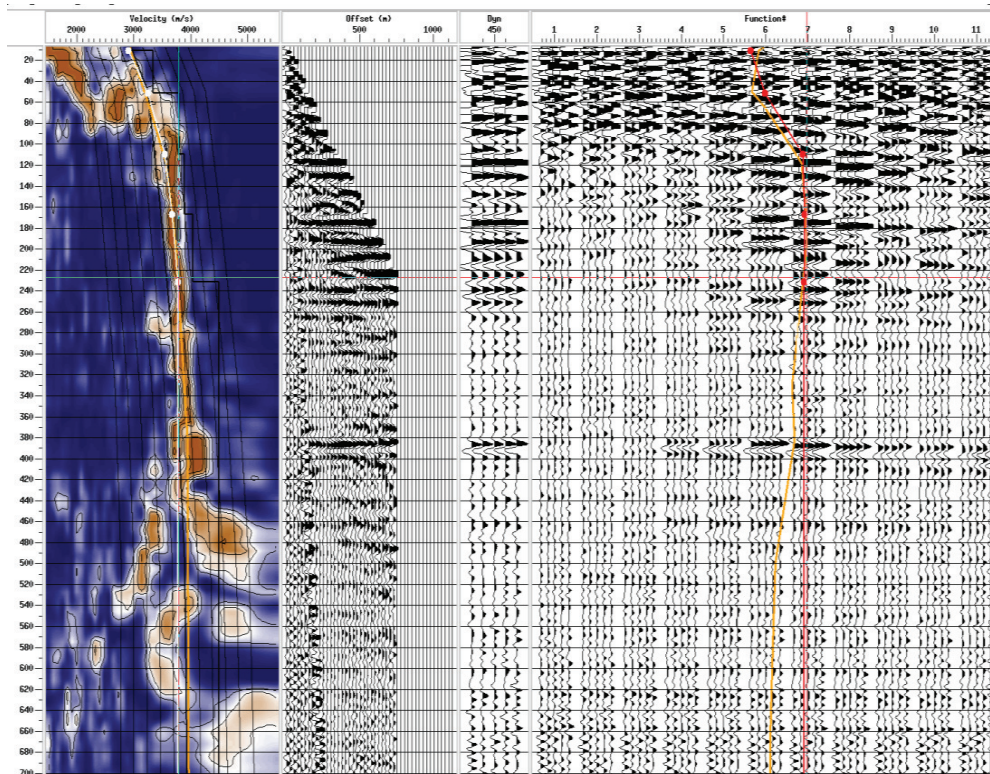


Figure A4. An example showing interactive velocity analysis display.

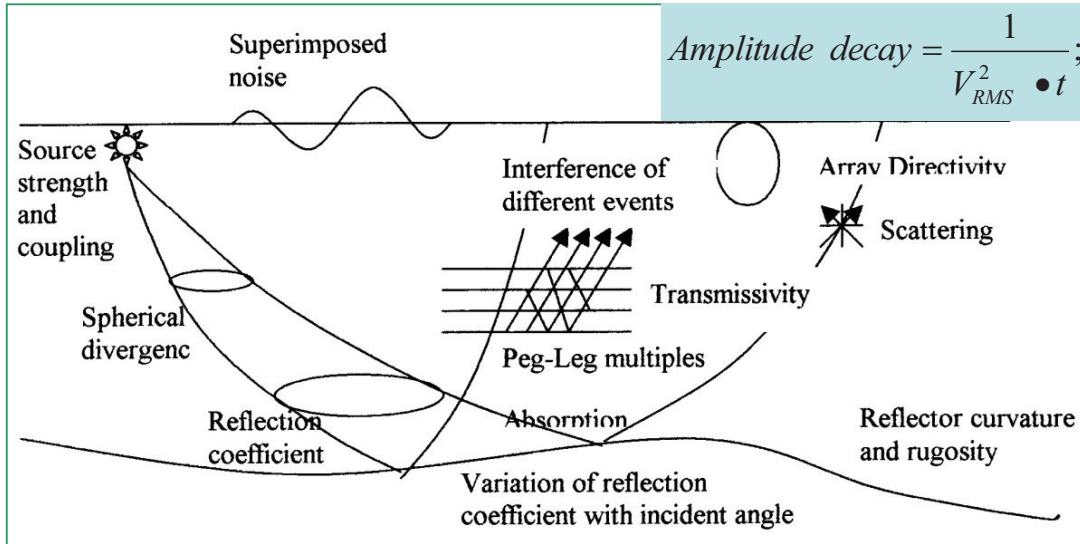


Figure A5. Various mechanisms causes seismic waves to gradually lose their energy. Spherical divergence is a consequence of the wavefront spreading, resulting in natural reduction of energy density with depth or time. The spreading rate is proportional to wave velocity. Correction is shown in blue box.

Energy partitioning

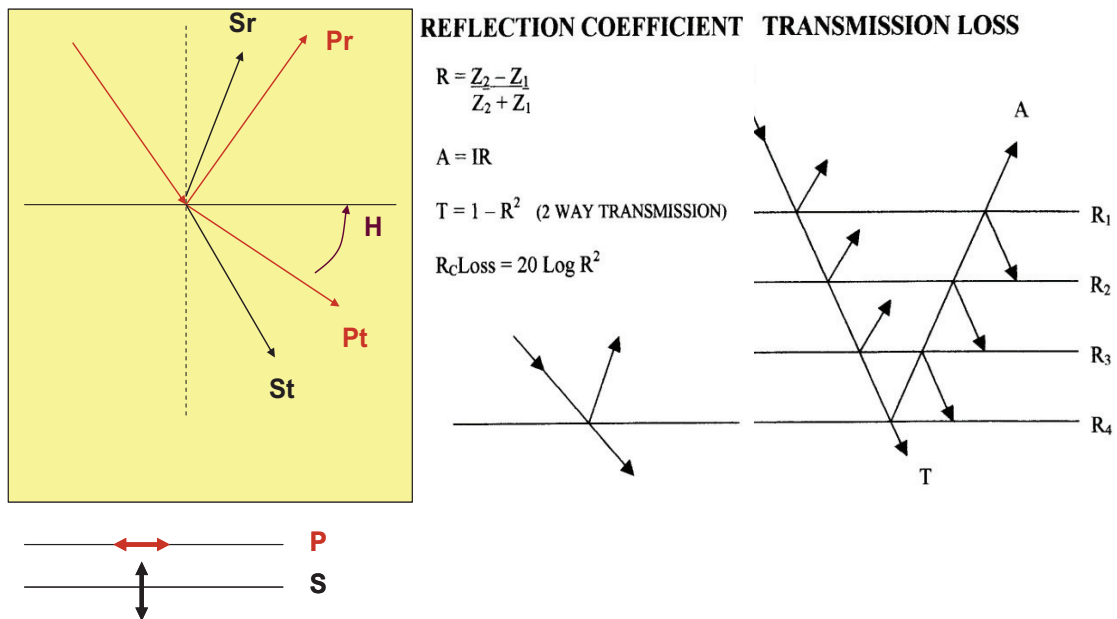


Figure A6. Reflection energy can be greatly decreased if the sedimentary section contains units which posses strong contrast in elastic properties. Then the amount of energy dissipated via refractions, reflections and mode conversions can be exceptionally large. In such case more powerful seismic sources may be required. This type of correction that is compensation is usually empirical. Parameters are determined by visual estimates.

Signal and noise

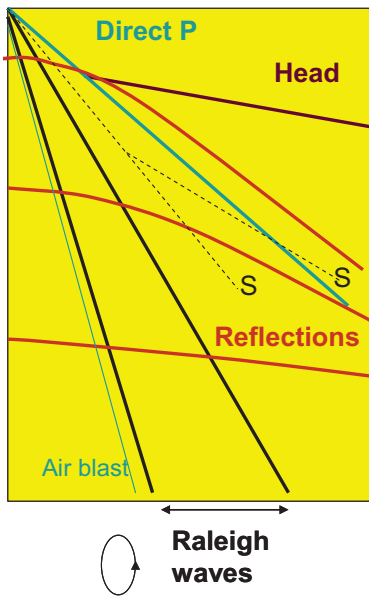
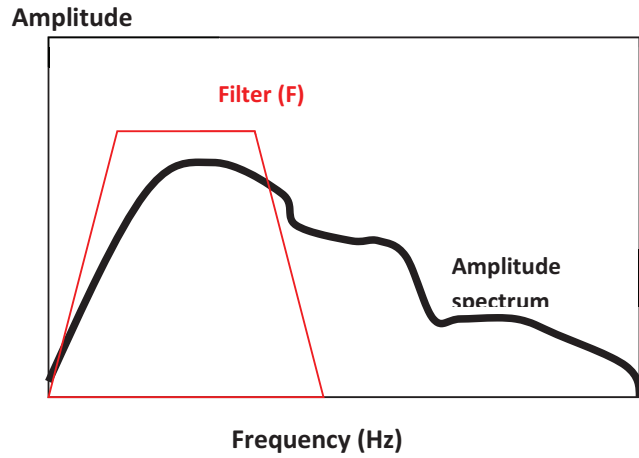


Figure A7. Various coherent noise trains generated by the source or by conversion at geological interfaces.

We aim to remove or attenuate all events but reflected primary waves.

Filtering (band-pass)



$$\text{Filtered trace} = \text{FFT}^{-1}(S \times F)$$

Figure A8. Real part of the forward Fourier transform of a seismic trace produces amplitude spectrum. Multiplication is the frequency domain with a trapezoid and inverse Fourier transform yields band-pass filtered seismic trace. In time domain this is equivalent to convolving seismic trace with a Sinc-function.

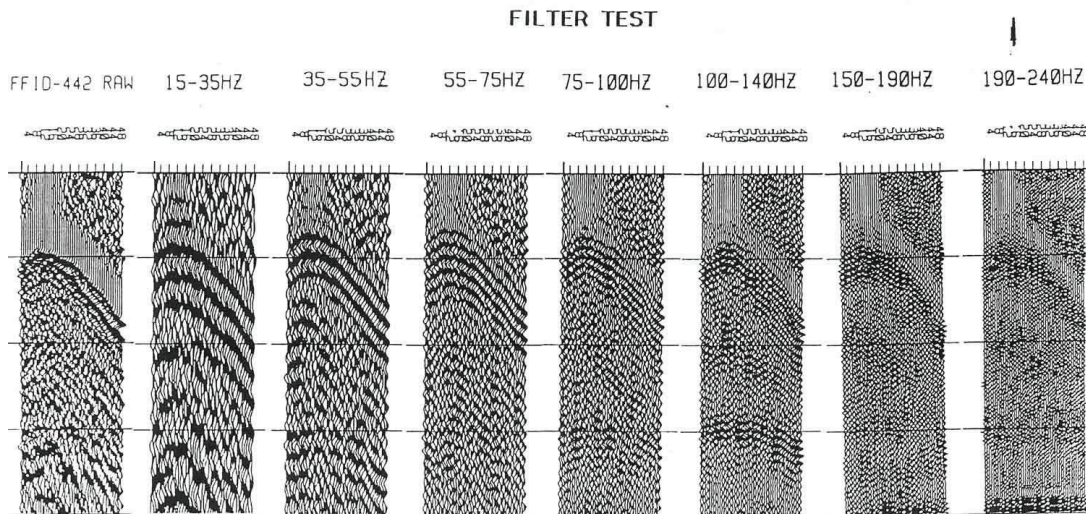


Figure A9. Estimation of the frequency content of the primary signal is usually accomplished by visual inspection of a narrow-band filtered record. Both the low-cut and the high-cut filter points are determined with such tests.

F-K filtering

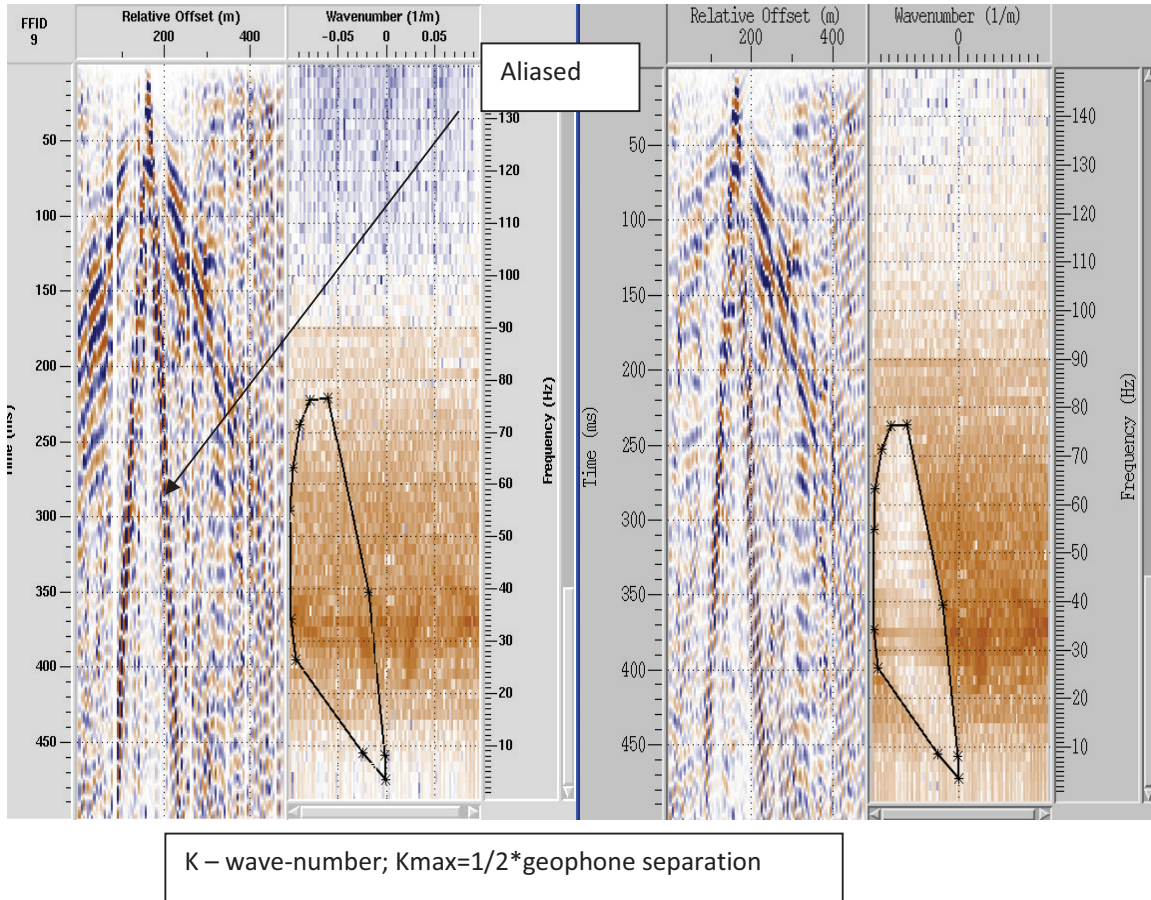


Figure A10. Two-dimensional Fourier transform is the basis for multi-channel filtering. In this domain events separate by the apparent velocity and frequency content. The reason is that an even with apparent slope α maps into frequency-wavenumber domain with slope $90-\alpha$. Piece-slice, velocity or polygonal (shown here) type of filtering is often used to attenuate coherent noise which has low apparent velocity. This is typically not possible for air blast which has a wide frequency content and velocity too low to allow for adequate spatial sampling.

Deconvolution

A seismogram is the convolution of the source wavelet w , with the earth's impulse e (defined by the reflection coefficient $R=z^2-z_1/z_2+z_1$), plus noise. That can be represented as:

$$x = w * e + n(t)$$

Optimum Wiener Filtering

$$\begin{bmatrix} r_0 & r_1 & \dots & r_{n-1} \\ \cdot & \cdot & \cdot & r_{n-2} \\ \cdot & \cdot & \cdot & \cdot \\ r_{n-1} & r_{n-2} & \dots & r_0 \end{bmatrix} \begin{bmatrix} a_0 \\ a_1 \\ \cdot \\ a_{n-1} \end{bmatrix} = \begin{bmatrix} g_0 \\ g_1 \\ \cdot \\ g_{n-1} \end{bmatrix}$$

Autocorrelation of the input wavelet

Desired filter coeff.

Cross-correlation of the desired output with the input wavelet

There are five choices of desired outputs:

Type 1. Zero-lag spike (Spiking Deconvolution)

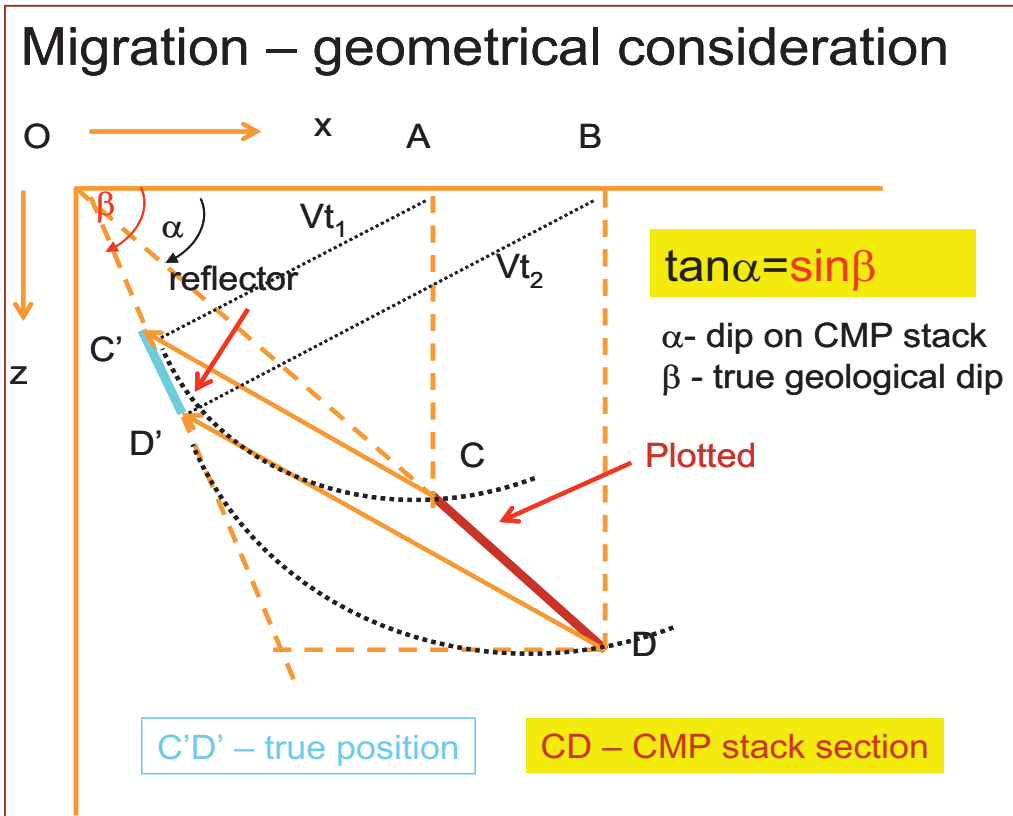
Type 2. Spike at arbitrary lag

Type 3 Time advanced form of input series (Predictive Deconvolution)

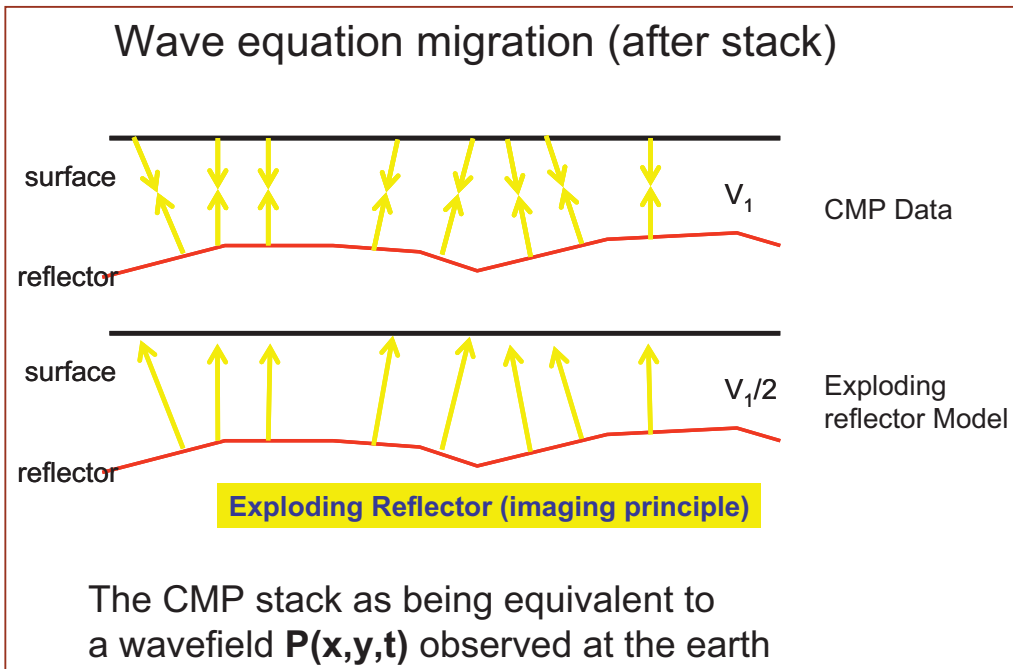
Type 4 Zero phase wavelet

Type 5 Any desired arbitrary shape

Figure A12. Principles of deconvolution and computations required.



a)



b)

Figure A13. Repositioning of seismic reflection energy into its “true” spatial position: a) geometrical aspect of migration and b) imaging principle (exploding reflector) commonly used for wave equation based migration techniques after stack.

Dip Move-Out Correction

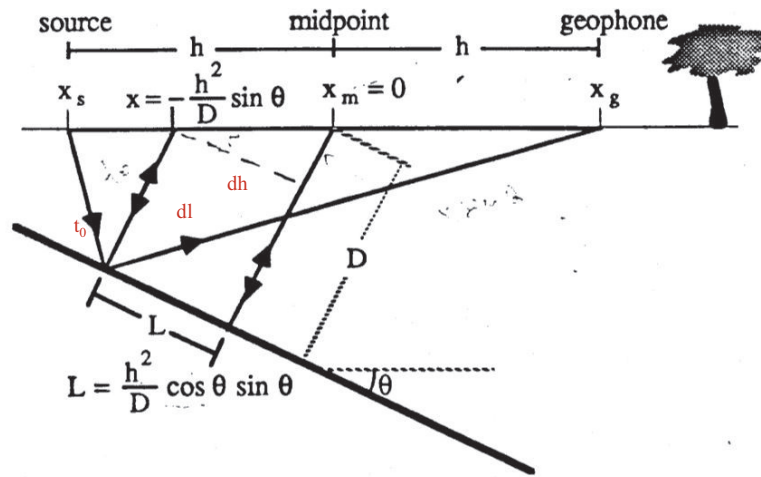
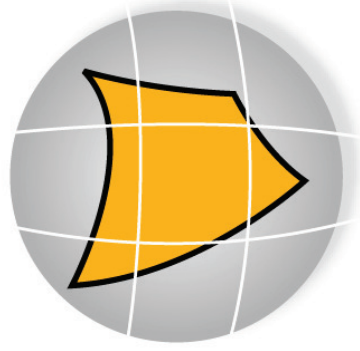


Figure A14. Reflection point displacement for a single dipping reflector. DMO process moves no zero-offset reflection to a midpoint. In this way common midpoint gather (CMP) becomes common reflection point gather. DMO correction is particularly important for hard rock seismic data processing.

APPENDIX E: PDA SURVEY REPORT

SURVEYING THE GRID

An outline of how the geophones
and shots were located.



PDA Surveyors

PDA Surveyors were faced with the objective to locate the geophones and shot holes to an accuracy of $0.1 \pm$ metres. They were spaced approximately 10 to 20 metres apart on a 100 by 100 metre grid covering an area of 1 by 1.5 kilometres.

Modern GPS receivers can easily achieve an accuracy of 30mm in open areas. However GPS will not achieve 0.1 metres accuracy under trees.



GPS suitable terrain

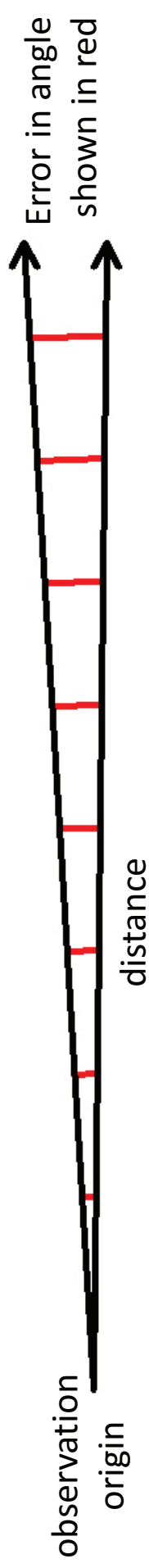


Traversing in harsh terrain

Traversing with total station was necessary where GPS was unable to achieve the accuracy required, which presents a number of obstacles.



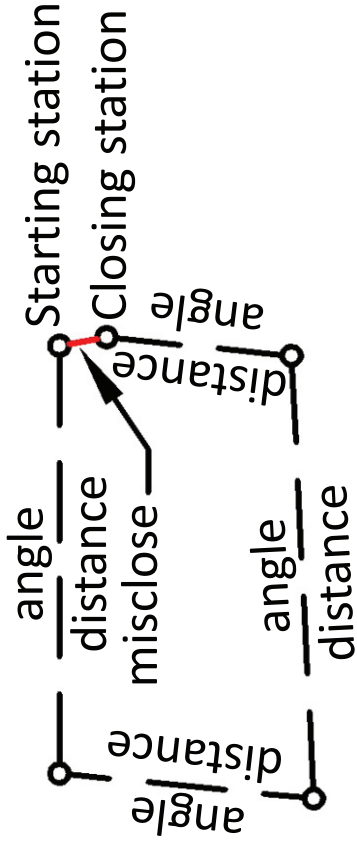
A total station observes horizontal and vertical angles and a slope distance to calculate a coordinate. Due to the soft ground, steep terrain, short lines of sight and at times poor visibility, errors in both horizontal and vertical angles become a problem in achieving the 0.1 accuracy. Errors in angles diverge with distance.



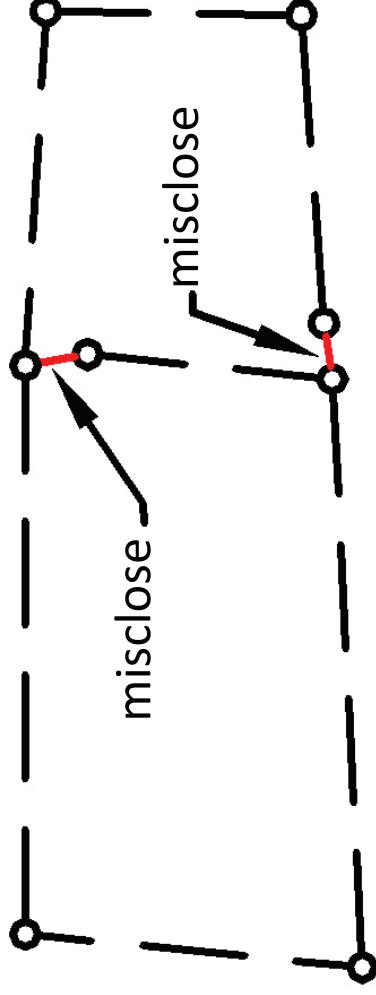
A typical example of implementing best survey practice. Ideally the total station should be set up on a stable surface to minimise possible errors.



Standard survey practice involves closing a traverse/loop allowing the determination of a misclose. A traverse would involve starting on a survey station, traversing around a loop and closing back onto the closing station. Theoretically the observed closing station coordinates would be the same as the starting station coordinates. This is rarely the case especially in the conditions on Mt Black.



The purpose of determining the misclose is so that the magnitude of error can be determined then mathematically adjusted so that the misclose becomes zero. When there is more than one loop it creates a network traverse. Network traverses are more complex to adjust as there are multiple solutions.



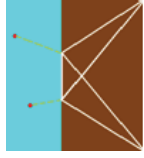
The solution is to implement least squares, which uses equations to minimise residuals. A residual is the difference between the original observation and the calculated value. Least squares determines the best possible result by distributing any errors throughout the network traverse. The adjustment allows for GPS observations to be integrated with the traverse observations, and for observations to be weighted. Most errors in the network have come from angles so larger adjustments were made in the angles and small adjustments to distances.

A matrix is used in the equations to minimise residuals. The matrix is the size of the number of observations adjusted. Consequently it is only recent that computers have had the processing power to be able to perform a least squares adjustment on a network traverse the size of what has been achieved on Mt Black.

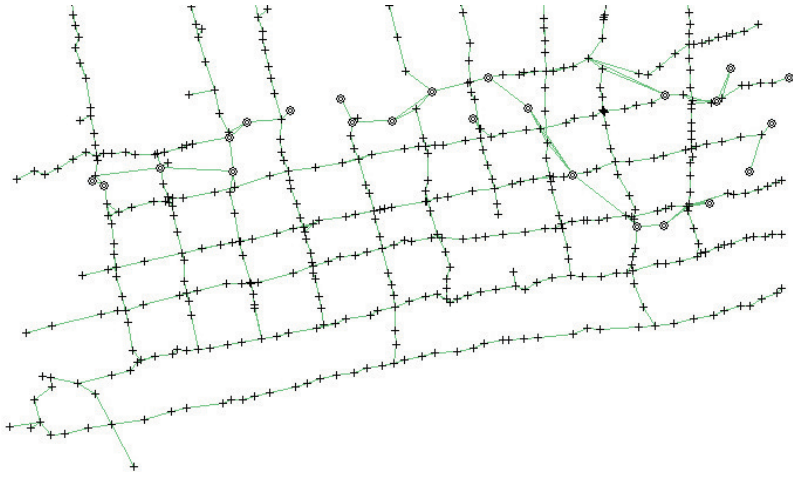
```
0 0 0 0 0
0 0 0 0 0
0 0 0 0 0
0 0 0 0 0
0 0 0 0 0
```

An example of a 5 by 5 matrix. The matrix in the least squares equation would be this small if there were only 5 observations to adjust. One adjustment had a matrix 4263 by 4263.

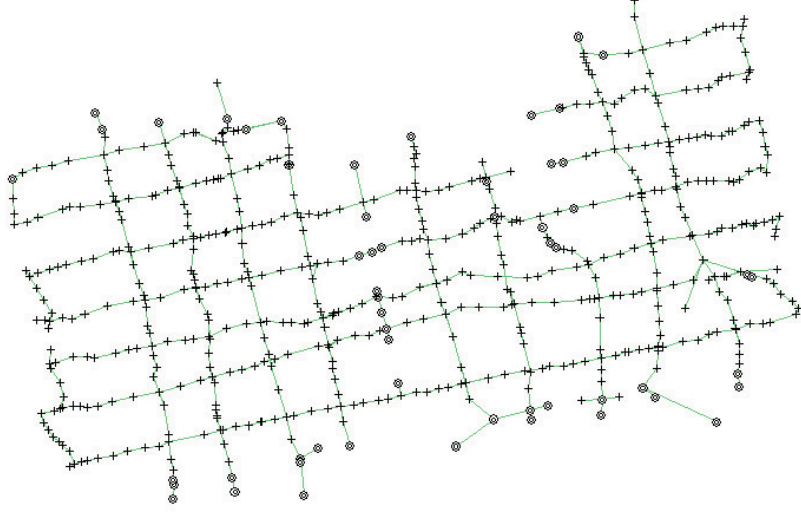




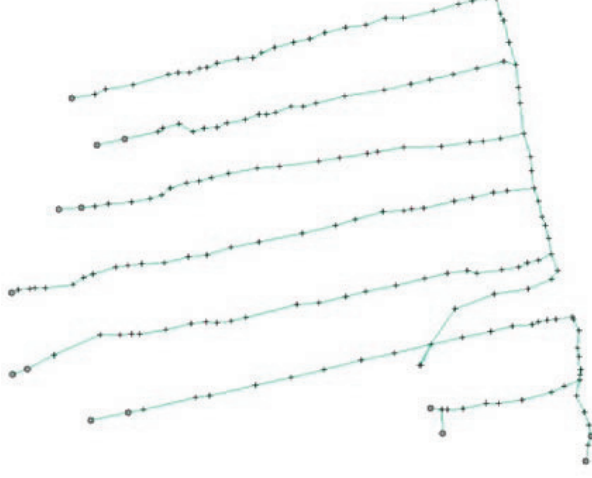
Screen shots from COMPNET least squares adjustment software. The ability of this software has been commendable in its ability to perform such large adjustments.



Network traverse west of
access road. 4263
observations adjusted.



Network traverse east
of access road. 3912
observations adjusted.

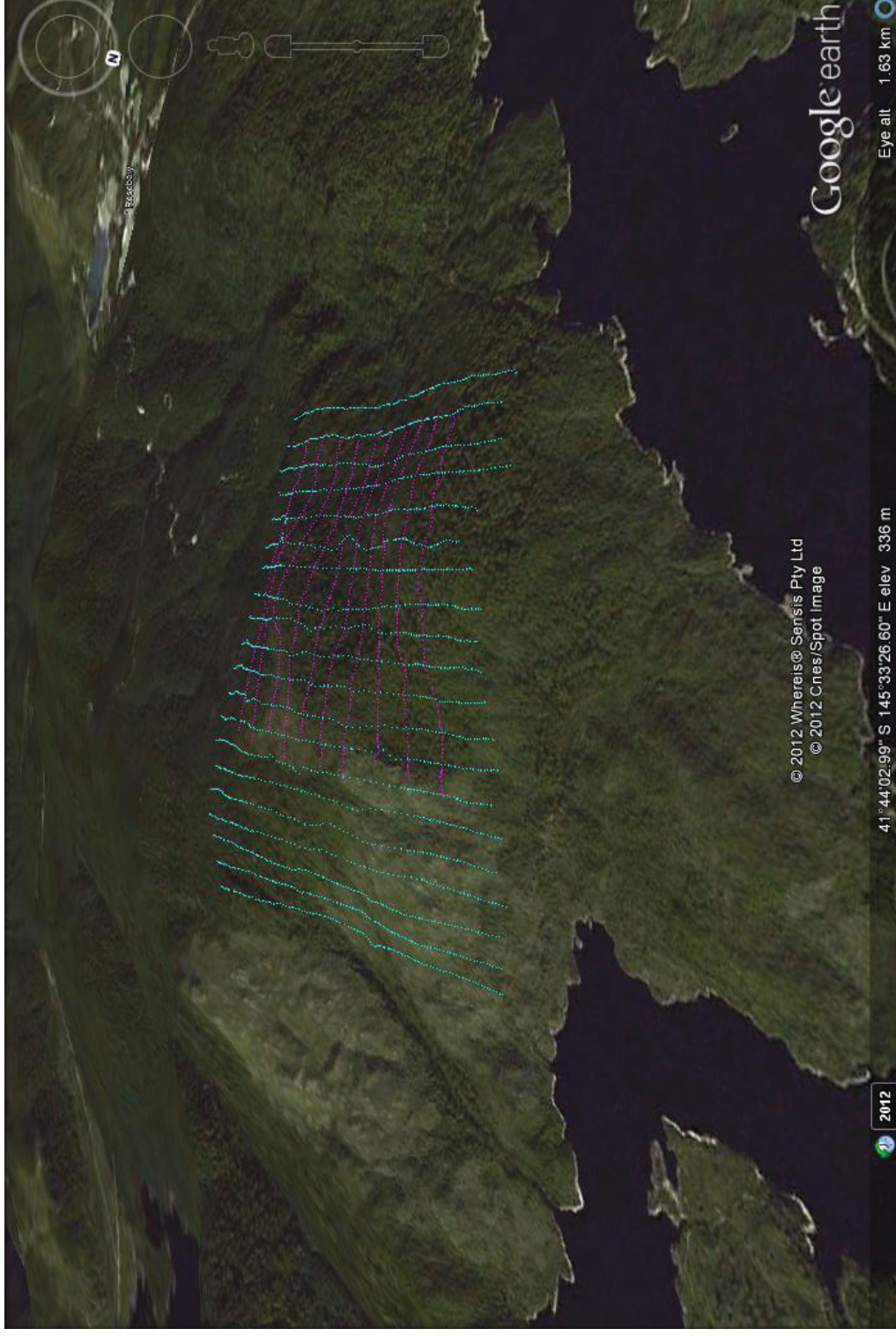


Traverse lines from shot
line 14 to 20. 1095
observations adjusted.

The result was 1963 shot holes and 961 geophones located. Taking 1266 traverse stations over 32+ kilometers of traverse and 9270 adjusted observations.



PDA Surveyors resources enabled us to complete the task in a timely manner with competent and committed staff. Our ability to use Compnet least squares software package allowed us to achieve the most accurate locations possible.



Google Earth overlay of geophones and shot holes as viewed looking to the south.



APPENDIX F: REFERENCES

3D Seismic Exploration for Mineral
Deposits in Hardrock Environments
E. L'Heureux, B. Milkereit and E. Adam
University of Toronto, Toronto, Canada
CSEH Recorder, November 2005

Salisbury, M., and Snyder, D., 2007, Application of seismic methods to mineral exploration, in Goodfellow, W.D., ed.,
Mineral Deposits of Canada: A
Synthesis of Major Deposit-Types, District Metallogeny, the Evolution of Geological Provinces, and Exploration
Methods: Geological Association of Canada,
Mineral Deposits Division, Special Publication No. 5, p. 971-982.